


RESEARCH

Open Access



# Exploring multi-omics and clinical characteristics linked to accelerated biological aging in Asian women of reproductive age: insights from the S-PRESTO study

Li Chen<sup>1,2\*</sup> , Karen Mei-Ling Tan<sup>1,3\*</sup>, Jia Xu<sup>1†</sup>, Priti Mishra<sup>1</sup>, Sartaj Ahmad Mir<sup>2,4</sup>, Min Gong<sup>1</sup>, Kothandaraman Narasimhan<sup>1</sup>, Bryan Ng<sup>1</sup>, Jun Shi Lai<sup>1</sup>, Mya Thway Tint<sup>1</sup>, Shirong Cai<sup>1,5</sup>, Suresh Anand Sadananthan<sup>1</sup>, Navin Michael<sup>1</sup>, Jadegoud Yaligar<sup>1</sup>, Sambasivam Sendhil Velan<sup>1,6</sup>, Melvin Khee Shing Leow<sup>1,7,8,9,10</sup>, Kok Hian Tan<sup>9,11</sup>, Jerry Chan<sup>9,11</sup>, Michael J. Meaney<sup>1,12,13</sup>, Shiao-Yng Chan<sup>1,10</sup>, Yap Seng Chong<sup>1,10</sup> and Johan G. Eriksson<sup>1,10,14,15</sup>

## Abstract

**Background** Phenotypic age (PhenoAge), a widely used marker of biological aging, has been shown to be a robust predictor of all-cause mortality and morbidity in different populations. Existing studies on biological aging have primarily focused on individual domains, resulting in a lack of a comprehensive understanding of the multi-systemic dysregulation that occurs in aging.

**Methods** PhenoAge was evaluated based on a linear combination of chronological age (CA) and 9 clinical biomarkers in 952 multi-ethnic Asian women of reproductive age. Phenotypic age acceleration (PhenoAgeAccel), an aging biomarker, represents PhenoAge after adjusting for CA. This study conducts an in-depth association analysis of PhenoAgeAccel with clinical, nutritional, lipidomic, gut microbiome, and genetic factors.

**Results** Higher adiposity, glycaemia, plasma saturated fatty acids, kynurenine pathway metabolites, GlycA, riboflavin, nicotinamide, and insulin-like growth factor binding proteins were positively associated with PhenoAgeAccel. Conversely, a healthier diet and higher levels of pyridoxal phosphate, all-trans retinol, betaine, tryptophan, glutamine, histidine, apolipoprotein B, and insulin-like growth factors were inversely associated with PhenoAgeAccel. Lipidomic analysis found 132 lipid species linked to PhenoAgeAccel, with PC(O-36:0) showing the strongest positive association and CE(24:5) demonstrating the strongest inverse association. A genome-wide association study identified rs9864994 as the top genetic variant ( $P = 5.69E-07$ ) from the *ZDHH19* gene. Gut microbiome analysis revealed that Erysipelotrichaceae UCG-003 and *Bacteroides vulgatus* were inversely associated with PhenoAgeAccel. Integrative network analysis of aging-related factors underscored the intricate links among clinical, nutritional and lipidomic variables, such as positive associations between kynurenine pathway metabolites, amino acids, adiposity, and insulin resistance.

<sup>†</sup>Li Chen, Karen Mei-Ling Tan and Jia Xu contributed equally to this work.

\*Correspondence:

Li Chen

chen\_li@sics.a-star.edu.sg

Karen Mei-Ling Tan

karen\_tan@sics.a-star.edu.sg

Full list of author information is available at the end of the article



Furthermore, potential mediation effects of blood biomarkers related to inflammation, immune response, and nutritional and energy metabolism were observed in the associations of diet, adiposity, genetic variants, and gut microbial species with PhenoAgeAccel.

**Conclusions** Our findings provide a comprehensive analysis of aging-related factors across multiple platforms, delineating their complex interconnections. This study is the first to report novel signatures in lipidomics, gut microbiome and blood biomarkers specifically associated with PhenoAgeAccel. These insights are invaluable in understanding the molecular and metabolic mechanisms underlying biological aging and shed light on potential interventions to mitigate accelerated biological aging by targeting modifiable factors.

**Keywords** Biological aging, PhenoAge, Age acceleration, GWAS, Lipidomics, Gut microbiome

## Background

Aging is a complex biological process characterized by several hallmark features such as chronic inflammation, genomic instability, epigenetic alterations, cellular senescence and mitochondrial dysfunction, leading to deterioration in function [1]. It is one of the leading risk factors for many chronic diseases such as type 2 diabetes, cardiovascular disease, dementia, and cancer [2, 3]. Thus, in a rapidly aging society, research into the mechanisms underlying aging can provide insights into how to extend healthy longevity by delaying the onset of age-related diseases. Biological aging is an increase in the rate of decline in physiological systems and functional ability that involves multiple organs and is gradual and progressive [4, 5]. While everyone ages chronologically at the same rate, substantial variance exists in biological aging. Thus, the identification of early life biomarkers to identify individuals at risk of accelerated biological aging may help in the prevention of age-related chronic diseases. Generally, women live longer and have lower biological ages than men, however there is a mortality-morbidity paradox where women on average appear to have poorer health in later life [6]. Hence, to address this paradox and promote healthy aging, there is a need to understand the fundamental cellular and molecular mechanisms of biological aging in women to prevent morbidity in older age.

Many biomarker assays have been developed to measure biological aging, such as the epigenetic clock [7], telomere length, metabolomics-based scores, and composite clinical biomarkers. There is no perfect gold-standard biological aging clock, however, composite clinical biomarkers representing a manifestation of multifactorial aging processes, have shown better predictive performance in morbidity and mortality than other markers such as the epigenetic clock [8, 9]. Most composite clinical biomarkers incorporate routine clinical biomarkers [10], and may include physiological clinical measures such as body mass index (BMI), blood pressure, hand grip strength and lung function [11, 12].

A measure of biological age, known as Phenotypic Age or PhenoAge, was developed using clinical data from the

third National Health and Nutrition Examination Survey (NHANES) [13], and validated in the fourth NHANES [9]. PhenoAge incorporates composite routine clinical haematology and chemistry biomarkers (albumin, creatinine, glucose, C-reactive protein (CRP), lymphocyte percent, mean red cell volume, red cell distribution width, alkaline phosphatase, and white blood cell count) based on parametrization from a Gompertz mortality model and was optimized to differentiate mortality risk among persons of the same chronological age (CA) [9, 13]. PhenoAge was shown to be a robust predictor of aging outcomes, strongly predicting risk of all-cause mortality in large cohorts, and in the general US population [9, 13]. BioAge, was another measure of biological age based on CA and 7 biomarkers including albumin, alkaline phosphatase, creatinine, C-reactive protein, glycated hemoglobin (HbA1c), SBP, and total cholesterol [10]. It was also trained in the third NHANES for mortality prediction. Compared to BioAge, PhenoAge performed better for prediction of mortality among healthy individuals [9]. In this study, we selected PhenoAge as the measure of biological aging as it uses routine clinical biomarkers that are readily available and can predict mortality and morbidity risk for healthy people. PhenoAge has been applied to Asian populations [14, 15] and showed a high correlation with CA ( $R=0.8\sim0.96$ ). PhenoAge was shown to predict mortality in Chinese patients with multi-vessel coronary artery disease [14]. Several studies have examined the association of lifestyle factors with PhenoAge [16, 17]. Genome-wide association studies of PhenoAgeAccel (PhenoAge after adjusting for CA) have been reported using data from the UK biobank [18] and Taiwan biobank [15] cohorts. One common genetic variant (rs1260326) in the *GCKR* (glucokinase regulator) gene was found in both studies.

Although aging is characterized by the simultaneous dysregulation of multiple systems, most studies on biological aging focus on a single system. To comprehensively understand the physiological and molecular aspects of biological aging, an integrative and multifaceted approach is essential. Moreover, few studies have

focussed on women alone, and the majority of studies predominantly featured Caucasian populations. The Singapore Preconception Study of Long-Term Maternal and Child Outcomes (S-PRESTO) longitudinal preconception cohort, a deeply-phenotyped, multi-ethnic cohort of Asian women of reproductive age, provides a promising opportunity to address these research gaps. We chose to study relatively young Asian women in order to characterize the pre-disease state, before the tipping point, where disease progression is still reversible [19]. To deepen our understanding of the mechanisms of biological aging in Asian women, we investigated the association of PhenoAgeAccel with various factors, including clinical, nutritional, lipidomic, gut microbiome and genetic factors. Furthermore, we applied an integrative network analysis to unveil potential biological pathways associated with biological aging.

## Methods

### Study population

Participants were from S-PRESTO (registered on ClinicalTrials.gov as NCT03531658), a prospective preconception cohort study in Singapore that recruited 1032 Chinese, Malay or Indian (or any combination thereof) women aged 18–45 years, attempting to conceive within the next 12 months, from February 2015 to October 2017 [20]. The S-PRESTO study was designed to examine the influences of events in the pre-conceptual period and early pregnancy on metabolic and mental health outcomes for both mother and offspring in later life. The primary outcomes were offspring adiposity and neurocognitive and behavioural development. The secondary outcomes included gestational age, mode of delivery, offspring and maternal metabolic and mental health. Women who were currently pregnant, were using oral or implanted contraception, or who were undergoing fertility treatment (apart from those taking clomiphene or letrozole alone in the past 1 month) were excluded from the study. Women with health conditions including established diabetes, on systemic steroids, anticonvulsants, HIV or Hepatitis B or C medication in the past 1 month were also excluded. The cohort profile has been described in detail [20]. This study was conducted according to the guidelines laid down in the Declaration of Helsinki. Ethics approval was obtained from the SingHealth Centralized Institute Review Board (reference 2014/692/D). All participants provided written informed consent.

### Clinical characteristics of participants

At the baseline visit, information on sociodemographic characteristics, obstetric history and lifestyle factors was obtained, together with measurements of weight, height,

waist and hip circumference, blood pressure (BP) and fasting blood collection. A fecal collection kit was also provided to the participants to return to the laboratory by courier. Ethnicity was based on self-reported parental ethnic group and coded as Chinese, Malay, Indian or mixed ethnicity. Education was assessed by the highest attainment of academic level, classified as below, or at/above university levels. Physical activity was evaluated using metabolic equivalent task scores in minutes (MET-minutes) using data obtained from an accelerometer (Actigraph wGT3X-BT) worn over 7 days. Time in physical activity was calculated using prediction equations according to Hildebrand et al. [21]. The Pittsburgh Sleep Quality Index (PSQI) was used to estimate sleep duration and quality [22]. The PSQI contains 19 items that generate 7 subcomponents scores (i.e., subjective sleep quality, sleep latency, sleep duration, habitual sleep efficiency, sleep disturbances, sleep medication, and daytime functioning) on a 0–3 scale and a summed global score ranging from 0 to 21; higher scores represent poorer subjective sleep quality. Dietary intake was assessed using a validated food frequency questionnaire [23], and healthy eating index (HEI) scores were calculated to reflect overall diet quality based on recommendations from the Singapore dietary guidelines for non-pregnant women [24]. Smoking exposure was defined as any active or passive cigarette smoking. Alcohol intake was assessed based on the consumption of any alcoholic beverage in the past three months.

Weight was measured using a SECA 803 weighing scale (Hamburg, Germany) to the nearest 0.1 kg; height was measured using a SECA 213 stadiometer (Hamburg, Germany) to the nearest 0.1 cm. Waist circumference was measured using a SECA 212 non-stretchable measuring tape (Hamburg, Germany), at the uppermost lateral border of the ilium. Blood pressure was measured on the right upper arm using a semi-automatic blood pressure monitor (Microlife BP 3AS1-2). All measurements were taken in duplicate and averaged. Body mass index (BMI) was calculated as weight (kg)/height (m)<sup>2</sup>. Body fat analysis was performed using air-displacement plethysmography on the Bod Pod™ Body Composition Tracking System (Cosmed, Rome, Italy). The participants wore the recommended form-fitting clothing and were weighed on a calibrated electronic scale. The mean of two measurements was used as the body volume and the fat mass (kg) and fat free mass (kg) were determined using the manufacturer's software (software version 5.2.0) [25].

The fat in the abdomen, liver, muscle, and pancreas was determined by magnetic resonance imaging (MRI) and spectroscopy (MRS) on Siemens Skyra 3 T MR scanner. The liver spectra were obtained from left and right lobes of the liver by point-resolved spectroscopy (PRESS)

sequence. The water and lipid peak areas were determined using LCModel [26] and used to estimate liver fat percentage by weight using validated methods [27]. The muscle spectra were obtained from the soleus and tibialis muscle compartments using PRESS sequence and processed using LCModel. The fat within the muscle fibres (intramyocellular lipids) was expressed as a percentage of the water signal. Abdominal fat was determined from axial image slices of the abdomen using 2-point Dixon sequence. Deep learn-

platform (Nightingale Health Ltd., Helsinki, Finland). These 9 biomarkers were combined with CA in the equation described in Liu et al. [9] to obtain phenotypic age.

$$\text{PhenotypicAge} = 141.50 + \frac{\ln[-0.00553 \times \ln(1 - M)]}{0.09165}$$

where

$$M = 1 - \exp\left(\frac{-1.51724 \times \exp(xb)}{0.0076927}\right)$$

---


$$\begin{aligned} xb = & -19.907 - 0.0336 \times \text{albumin} + 0.0095 \times \text{creatinine} + 0.1953 \times \text{glucose} + 0.0954 \times \ln(\text{CRP}) \\ & - 0.0120 \times \text{lymphocyte percent} + 0.0268 \times \text{mean cell volume} + 0.3306 \times \text{red blood cell distribution width} \\ & + 0.00188 \times \text{alkaline phosphatase} + 0.0554 \times \text{white blood cell count} + 0.0804 \times \text{chronological age} \end{aligned}$$


---

ing based automated segmentation was performed to segment and quantify subcutaneous (SAT) and visceral (VAT) adipose tissue depots between L1 and L5 vertebrae [28]. To estimate pancreatic fat, multiple regions of interest (ROIs) were selected within the pancreas (head-body and tail) in the fat fraction image obtained using 6-point Dixon sequence. The pancreatic fat was quantified as the mean proton density fat fraction within the selected ROIs.

Data concerning depressive and anxiety symptoms were collected through the administration of questionnaires [29]. Depressive symptoms were evaluated using the Edinburgh Postnatal Depression Scale (EPDS), which comprises ten questions about typical depressive symptoms experienced within the past week. Anxiety was assessed using the Spielberger State-Trait Anxiety Inventory (STAI), featuring 40 items graded on a 4-point Likert scale. Of these items, twenty were designated to measure the state of anxiety, capturing temporary anxiety characteristics (e.g., anxiety disorders), while the remaining twenty items assessed the trait aspect of anxiety, reflecting a more enduring personality trait such as an anxious disposition.

#### Derivation of PhenoAge acceleration

Mean red blood cell volume, red cell distribution width, white blood cell count, and lymphocyte percent were analysed in whole blood collected in EDTA blood tubes at the KK Women's and Children's hospital (KKH) clinical laboratory [20]. Fasting glucose was analysed in plasma from blood collected in fluoride blood tubes at the KK Women's and Children's hospital (KKH) clinical laboratory. Creatinine, C-reactive protein and alkaline phosphatase were analysed in serum on Alinity c (Abbott, Illinois, USA) at the National University Hospital (NUH) clinical laboratory. Albumin was measured in EDTA plasma using an automated nuclear magnetic resonance (NMR)-based high throughput metabolomics

Phenotypic age acceleration (PhenoAgeAccel) was calculated as the residuals resulting from the regression of phenotypic age on chronological age [9].

#### Blood biomarkers

A total of 70 biomarkers were measured in blood samples. They include lipid profile, liver enzymes, glycaemic measures, vitamins, metabolites, growth factors, fatty acids, amino acids, and protein biomarkers.

A clinical lipid panel (triglyceride, total cholesterol, HDL-cholesterol) and liver enzymes (alanine transaminase (ALT), aspartate transaminase (AST) and gamma glutamyl transferase (GGT)) were measured in serum samples using enzymatic colorimetric methods on AU5800 (Beckman Coulter, USA) at the National University Hospital (NUH) clinical laboratory. LDL-cholesterol was calculated using the Friedewald equation (LDL-cholesterol (mmol/L) = Total cholesterol (mmol/L) - HDL-cholesterol (mmol/L) - triglyceride (mmol/L) / 2.2). Fasting plasma glucose (FPG) and insulin concentrations were measured after an overnight fasting (8–14 h), and 2-h post-load glucose concentration (2hPG) was measured at two hours after taking 75 g of glucose. HOMA-IR was calculated by the mathematical equation (insulin (mU/mL) x FPG (mmol/L)/22.5) [30]. HbA1c was analysed in whole blood at the KK Women's and Children's hospital (KKH) clinical laboratory. Fasting insulin concentration was measured using immunoassay on Beckman Dxi 800.

Serum folate and vitamin B12 were measured on Access2 (Beckman Coulter, USA) at the NUH clinical laboratory. Other vitamins (thiamine, riboflavin, nicotinamide, pyridoxal phosphate, vitamin D, all-trans retinol, alpha tocopherol and gamma tocopherol), one carbon pathway metabolites (homocysteine, methionine, betaine, choline, dimethylglycine, cystathionine and cysteine), and tryptophan metabolites (tryptophan, kynurenine,



kynurenic acid, 2-hydroxylnurenine, xanthurenic acid, 3-hydroxyanthranilic acid, quinolinic acid and neopterin) were measured in EDTA plasma using a targeted liquid chromatography-tandem mass spectrometry platform (BEVITAL AS Ltd., Bergen, Norway). Growth hormone, insulin-like growth factors (IGF-1 and IGF-2) and insulin-like growth factor binding proteins (IGFBP-1, IGFBP-3, IGFBP-4, IGFBP-5, IGFBP-6 and IGFBP-7) were measured using a multiplex Luminex assay. Fatty acid (FA) measures (total FAs, degree of unsaturation, n-3 FAs (%), n-6 FAs (%), PUFAs (polyunsaturated FAs, %), MUFAs (monounsaturated FAs, %), SFAs (saturated FAs, %), LA (linoleic acid, %), DHA (docosahexaenoic acid, %) and two ratios: PUFAs / MUFAs and n-6 FAs / n-3 FAs), amino acids (alanine, glutamine, glycine, histidine, total concentration of branched-chain amino acids, isoleucine, leucine, valine, phenylalanine and tyrosine), apolipoproteins and glycoprotein acetyls (GlycA) were measured in EDTA plasma using the high-throughput proton Nuclear Magnetic Resonance (<sup>1</sup>HNMR) metabolomics (Nightingale Health, Helsinki, Finland).

#### Plasma lipidomics

High coverage quantitative lipidomics was performed as described previously [31]. Briefly, total lipids were extracted using a single-phase butanol: methanol (1:1, v/v) extraction solvent containing class specific internal standards. These lipid extracts were analysed by using Agilent 6495 QQQ mass spectrometer interfaced with an Agilent 1290 series HPLC system. Lipids were separated on a ZORBAX RRHD UHPLC C<sub>18</sub> column (2.1 × 100 mm 1.8 mm, Agilent Technologies) with temperature maintained at 45 °C. Mass spectrometry analysis was performed in ESI positive ion mode with dynamic multiple reaction monitoring (dMRM). QC samples were analysed along with the samples to monitor sample extraction efficiency as well as LC-MS performance and were subsequently used to do batch corrections. Lipid species were dropped if quality control coefficient of variation were greater than 25% after batch correction. Finally, a total of 689 plasma lipid species representing 36 lipid classes were used for the downstream data analysis.

#### Whole genome sequencing

DNA extraction, library preparation, sequencing and quality check were reported previously [32]. Briefly, samples were sequenced on the Illumina HiSeq 4000 platform (30 × and 2 × 150 bp). Samples failed by variant quality score recalibration (VQSR) were removed. Reads were aligned to human reference genome GRCh37 using BWA MEM (0.7.15) and duplicates were removed with sambamba (0.6.5). BAM files were processed with GATK version 4.0. Samples with cryptic relatedness, or

ethnic discrepancies were excluded. Bi-allelic SNPs were extracted for genome-wide association studies.

#### Gut microbiome

The fresh fecal samples were collected and delivered to the lab within 24 h with cold chain transportation and stored in the -80 °C freezer. The fecal genomic DNA was extracted from 250 mg feces using the Qiagen PowerFecal Pro Kit (QIAGEN, Inc., Netherlands). Amplification of the V4 region of the 16S rRNA gene was carried out with the updated 515F (Parada)—806R (Apprill) primer set (FWD-GTGYCAGCMGCCGCGGTAA; REV-GGACTA CNVGGGTWCTAAT) [33–35]. The jagged ends of DNA fragments were converted into blunt ends by using T4 DNA polymerase, Klenow Fragment and T4 Polynucleotide Kinase. Then an 'A' base was added to each 3' end to make it easier to add adapters. After all that, fragments too short were removed by AMPure beads. Paired-end sequencing of 2 × 250 bp was performed using the Illumina HiSeq 2500 platform (Illumina, San Diego, CA, USA) at BGI Genomics Co., Ltd (Shenzhen, China).

#### Statistical analysis

Out of 1032 women, 952 had blood collected for measurement, with a small proportion of women not fasted or refused blood collection or unable to collect blood. Finally, a total of 952 women were included in this study with available CA and the measures of nine biomarkers required in the equation of phenotypic age described in Liu et al. [9]. A subset of participants had available clinical, nutritional, lipidomic ( $N=923$ ), gut microbiome ( $N=630$ ) and genetic data ( $N=882$ ) after quality check. Sample sizes of clinical and nutritional data are listed in Additional file 1: Table S1-2. The flow chart of the study is shown in Fig. 1A. Normality was checked for all the continuous variables. As the distributions of some continuous variables were skewed, log<sub>10</sub> transformation was applied for further analysis. The association analyses with PhenoAgeAccel were performed using IBM SPSS Statistics v26 and MATLAB 2022b.

#### Clinical analysis

Linear regression was used to study the association between PhenoAgeAccel (outcome) and clinical variables (predictors) using univariate and multivariate analyses. For continuous predictors, z-scores of predictor variables were used in regression analysis, and the effect sizes  $\beta$  were reported as years of age acceleration per SD change in predictors. For categorical predictors (i.e., ethnicity, educational attainment, smoking status, alcohol assumption and parity), the effect sizes  $\beta$  were reported as difference in years of age acceleration between groups. Age, BMI, ethnicity, educational attainment and parity were

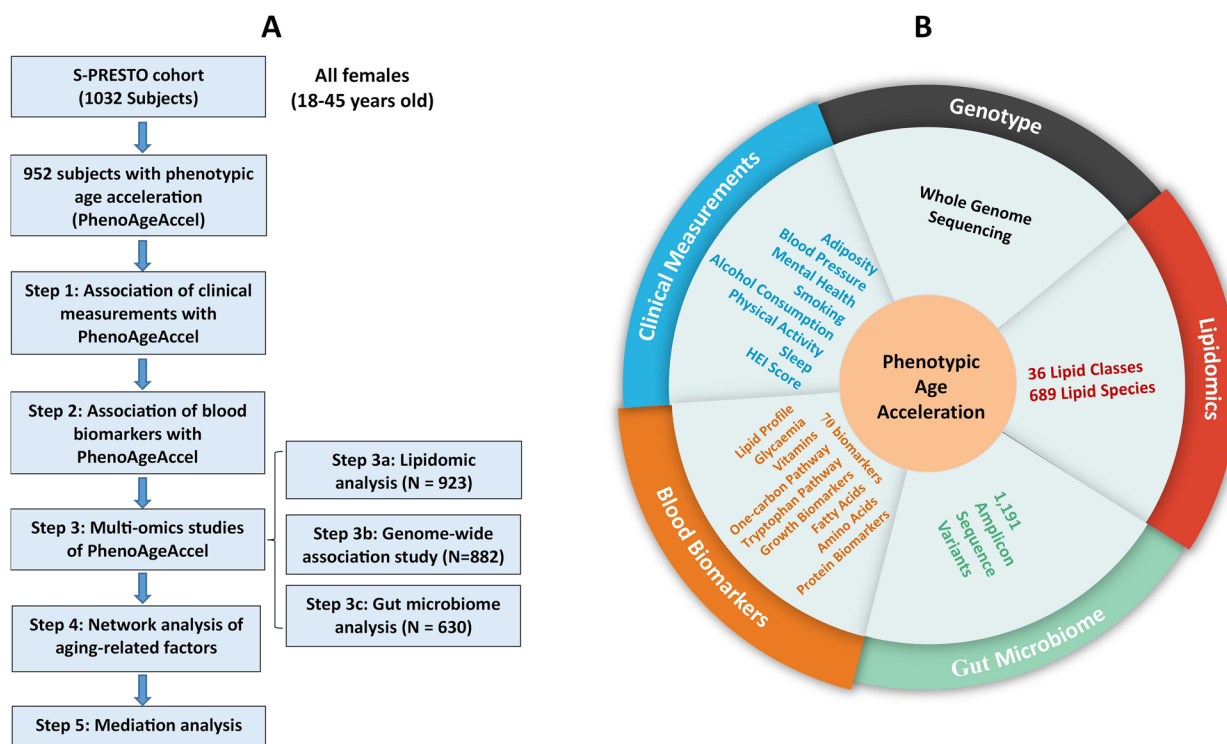


**Fig. 1** The phenotypic age acceleration (PhenoAgeAccel) study. **A** A flow chart of sample selection and analysis steps. **B** A diagram illustrating the investigation of PhenoAgeAccel through the integration of clinical measurements, blood biomarkers and multi-omics

adjusted in multivariate analysis. The participants with missing values were excluded in the analysis of each factor. The adjusted  $p$ -values ( $P_{adj}$ ) were calculated by the Benjamini-Hochberg (BH) method for multiple testing correction.

**Lipidomic analysis**

Plasma lipidomics data based on LC-MS/MS quantification were  $\log_{10}$  transformed for analysis. The association analysis was applied between the log-transformed lipidomic data and PhenoAgeAccel by linear regression after the adjustment for age, ethnicity, educational attainment, parity and BMI (N = 923). The regression coefficients ( $\beta$ ) were converted to % change in lipid concentration per year of age acceleration ( $\% \text{ change} = (10^\beta - 1) \times 100$ ). The adjusted  $p$ -values ( $P_{adj}$ ) were calculated by the Benjamini-Hochberg (BH) method for multiple testing correction.

**Genome-wide association studies (GWAS)**

Several participants with mixed ethnicity were excluded from this analysis. In total, 882 subjects (667 Chinese, 134 Malay and 81 Indian) were studied in this GWAS analysis. SNPs with call rates less than 95% or minor allele frequency (MAF) less than 5% or Hardy-Weinberg equilibrium (HWE)  $P$  value less than  $1.00E-06$  were

excluded. Finally, 5,835,822 SNPs were used for GWAS. The genotypes of each genetic variant were coded as 0-AA, 1-Aa and 2-aa using additive model (A- reference allele and a- alternate allele). The association between the coded genotype data and PhenoAgeAccel were studied in regression analysis after the adjustment of age and ethnicity. The effect size is denoted in years of age acceleration per dosage change of effect allele (alternate allele). GWAS was performed in PLINK 1.9.

**Gut microbiome analysis**

The initial raw sequencing data underwent processing using DADA2 to obtain the number of Amplicon Sequence Variant (ASV) in each sample [36]. Taxonomic classifications for each ASV's representative sequence were assigned employing a Naive Bayes classifier trained on the V4 region of the 16S rRNA gene with the SILVA database v138.1 in QIIME2 [37, 38]. The phylogenetic tree was constructed with the SEPP method within the fragment-insertion plugin [39]. A total of 630 women contributed fecal samples for 16S rRNA gene V4 region sequencing, resulting in a dataset comprising 54,129,873 high-quality reads. The sequencing depth averaged  $85,920 \pm 25,339$  reads per sample. In total, 1,191 ASVs were obtained for subsequent analysis. To mitigate discrepancies arising from varying sequencing depths

among the samples, the abundances of ASVs in each sample underwent rarefaction to a standardized depth of 20,000 reads per sample for subsequent analysis. The diversity plugin in QIIME2 was utilized for the generation of alpha-diversity indices, beta-diversity distance matrices, and ordination matrices through the core-metrics-phylogenetic method. Multi-way ADONIS permutation-based statistical test was applied to determine whether gut microbiome was associated with PhenoAgeAccel after adjusting for the effects of covariates in vegan-R. The gut microbes associated with PhenoAgeAccel were identified using a Random Forest Regressor with q2-sample-classifier [40], which involved a nested stratified tenfold cross-validation approach using 500 decision trees. The seed used by random number generator is 123. Association between alpha-diversity indices/microbial species and age acceleration adjusting for covariates was performed with MaAsLin2 [41].

### Network analysis

Integrative network analysis was performed based on Spearman's rank correlation coefficients using the Cytoscape software (version 3.10.1) [42]. Two networks were studied for (1) the interconnection between elements of PhenoAge and selected aging-related factors, and (2) the interconnection among aging-related factors. Pairwise correlation heat map was generated for the overview of their interconnection. To simplify the networks, the connections with a correlation coefficient of  $\geq 0.30$  were selected for network visualization. The correlation coefficients between them were used as the edge table. The factors were categorized based on their properties in the node table.

### Mediation analysis

Mediation analysis was performed to investigate the effects of candidate mediators on the associations between predictors and the outcome (PhenoAgeAccel) using the "mediate" function from the R package "mediation" (boot=TRUE, sims=1000, R version 4.4.1). First, mediation analysis was performed for 10 predictors (diet (HEI score), adiposity (fat mass, liver fat, and visceral adipose tissue), 3 genetic variants and 3 gut microbial species) and 36 candidate mediators (aging-related blood biomarkers). Second, mediation analysis of 7 predictors (diet, adiposity, and genetic variants) and 3 candidate mediators (gut microbial species) were investigated. Age, ethnicity, educational attainment, parity and BMI were adjusted in analysis models. Linear models were used in most of the analysis, except that generalized linear models were applied for gut microbial species. The results of average causal mediation effects (ACME), average direct effects, and total effect were reported. For each predictor,

the adjusted *p*-values were calculated by the Benjamini-Hochberg (BH) method for multiple testing correction.

## Results

### Participant characteristics and PhenoAgeAccel

Depending on the availability of key variables required for this study, data from 952 of 1032 women were analysed from the S-PRESTO cohort. PhenoAge of each participant was calculated based on CA and nine biomarkers (Additional file 1: Table S1 and Methods). Subsequently, PhenoAgeAccel was calculated as the residuals resulting from the regression of PhenoAge on CA. Clinical characteristics of all participants in this study are shown in Table 1. A flow chart outlining the steps for sample selection and data analysis is provided in Fig. 1A. The association with PhenoAgeAccel was investigated through the integration of clinical measurements, blood biomarkers, and multi-omics (Fig. 1B). In this study, the majority of the participants were Chinese (72%), with 63% having a university-level education and 65% being nulliparous. The mean PhenoAge (Mean  $\pm$  SD:  $26.91 \pm 6.68$ ) was lower than the mean chronological age ( $31.34 \pm 3.72$ ), with a strong correlation ( $R=0.52$ , Fig. 2A and Additional file 1: Fig. S1A). PhenoAgeAccel was fairly normally distributed ( $0.00 \pm 5.69$ , Fig. 2B) with some outliers in the positive (older) direction. Among all the participants, 427 (45%) exhibited an accelerated biological aging (positive PhenoAgeAccel), while 525 (55%) displayed a decelerated biological aging (negative PhenoAgeAccel). PhenoAgeAccel was slightly higher in older women ( $0.23 \pm 4.94$ ,  $N=140$ , aged  $\geq 35$  years) compared to younger women ( $-0.04 \pm 5.81$ ,  $N=812$ , aged  $< 35$  years), but the group difference was not statistically significant (Additional file 1: Fig. S1B).

Compared to Chinese women, Malay had a younger CA and a similar PhenoAge (Additional file 1: Fig. S1C), but a higher PhenoAgeAccel (Fig. 2C). Indian women had the highest PhenoAge (Additional file 1: Fig. S1C) and PhenoAgeAccel (Fig. 2C) amongst all the ethnicities. Higher educational attainment was associated with lower PhenoAgeAccel (Table 1 and Fig. 2D). Multiparous women (Mean  $\pm$  SD:  $0.21 \pm 5.82$ ) had a higher PhenoAgeAccel than nulliparous women ( $-0.10 \pm 5.63$ ), but the association was not strong (Table 1 and Fig. 2E). There was a strong positive association between BMI and PhenoAgeAccel (Fig. 2F). Specifically, PhenoAge was accelerated by 2.50 years per SD increase in BMI. Notably, this effect was mainly driven by variation in weight, as height was not associated with PhenoAgeAccel (Table 1). To account for the effects of potential confounding factors, chronological age, ethnicity, educational attainment, parity, and BMI were adjusted for further analysis.

**Table 1** Clinical characteristics of the participants in this study

Variable	N	Mean (SD) / %	Univariate Analysis*	
			$\beta$ (95% CI)	p-value
PhenoAgeAccel (years)	952	0.00 (5.69)	--	--
PhenoAge (years)	952	26.91 (6.68)	4.85 (4.64, 5.04)	<b>2.03E-269</b>
Chronological Age (years)	952	31.34 (3.72)	0.00 (-0.36, 0.36)	1.00
Ethnicity				
Chinese	686	72.06%	Ref	Ref
Malay	143	15.02%	3.40 (2.43, 4.37)	<b>1.24E-11</b>
Indian	88	9.24%	5.17 (3.97, 6.37)	<b>9.50E-17</b>
Mixed	35	3.68%	3.51 (1.67, 5.34)	<b>1.85E-04</b>
Educational Attainment				
Below University	352	37.01%	Ref	Ref
University	599	62.99%	-2.40 (-3.14, -1.67)	<b>2.23E-10</b>
Parity				
Nulliparous	616	64.84%	Ref	Ref
Multiparous	334	35.16%	0.31 (-0.45, 1.07)	4.26E-01
Weight (kg)	947	60.99 (13.79)	2.46 (2.13, 2.79)	<b>3.11E-44</b>
Height (cm)	946	159.89 (5.60)	0.15 (-0.21, 0.52)	4.17E-01
Body Mass Index (kg/m <sup>2</sup> )	946	23.86 (5.27)	2.50 (2.17, 2.83)	<b>1.26E-45</b>

\* Association analysis with PhenoAgeAccel

**Clinical factors associated with PhenoAgeAccel**

Both univariate and multivariate analyses of clinical measurements (i.e. adiposity, blood pressure, pregnant status within 12 months after recruitment, mental health, and lifestyle) were performed on PhenoAgeAccel (Additional file 1: Table S2). Effect size  $\beta$  was reported as years of age acceleration per SD change for continuous predictors or difference in years of age acceleration between groups for categorical predictors.

As for adiposity factors, fat mass ( $\beta=1.86$  and  $P=3.61E-03$ ), visceral adipose tissue ( $\beta=1.69$  and  $P=1.08E-04$ ) and liver fat ( $\beta=0.67$  and  $P=3.45E-02$ ) displayed a strong positive association with PhenoAgeAccel even after adjusting for covariates (Fig. 2G). Waist to hip ratio, fat free mass, subcutaneous adipose tissue, pancreatic fat, intramyocellular fat (tibialis anterior), intramyocellular fat (soleus) and blood pressure only exhibited a strong association in univariate analysis, but lost significance after adjusting for covariates. This study also explored the association between PhenoAgeAccel and mental health using the EPDS and STAI scores. No strong association was observed. The association of fertility with PhenoAgeAccel revealed that the women who conceived within 12 months after recruitment had lower PhenoAgeAccel ( $-0.51 \pm 5.58$ ) compared to those who did not conceive within the same timeframe ( $0.43 \pm 5.76$ ). However, this association was only significant in univariate analysis ( $\beta = -0.94$  and  $P = 1.22E-02$ ). Women who

were smokers had higher PhenoAgeAccel ( $\beta=1.99$  and  $P=8.12E-04$ ) compared to non-smokers, while women who were alcohol drinkers had lower PhenoAgeAccel ( $\beta=-1.07$  and  $P=7.37E-03$ ) compared to non-drinkers in univariate analysis, but the associations lost significance after adjusting for covariates. There was no observed association of PhenoAgeAccel with physical activity, sleep duration and sleep quality. A higher HEI score was associated with lower PhenoAgeAccel ( $\beta=-0.45$  and  $P=8.39E-03$ , Fig. 2G).

**Blood biomarkers associated with PhenoAgeAccel**

In this study, we investigated the association between PhenoAgeAccel and a wide range of biomarkers measured in serum or plasma (Additional file 1: Table S2). For glycaemic traits, since fasting glucose was one of the biomarkers included in the calculation of PhenoAge and contributed positively to it (Additional file 1: Table S1), higher levels of 2-h post-load glucose, fasting insulin, HbA1c and HOMA-IR were associated with accelerated biological aging, as expected. Serum triglyceride ( $\beta=0.97$  and  $P=1.42E-07$ ), LDL-cholesterol ( $\beta=0.42$  and  $P=2.18E-02$ ), liver enzymes (ALT:  $\beta=0.89$  and  $P=1.47E-06$  and AST:  $\beta=0.58$  and  $P=1.52E-03$  and GGT:  $\beta=1.22$  and  $P=3.06E-11$ ) showed a positive association with PhenoAgeAccel, while serum HDL-cholesterol had an inverse association with PhenoAgeAccel ( $\beta=-1.49$  and  $P=2.63E-16$ ) in univariate analysis; however, these



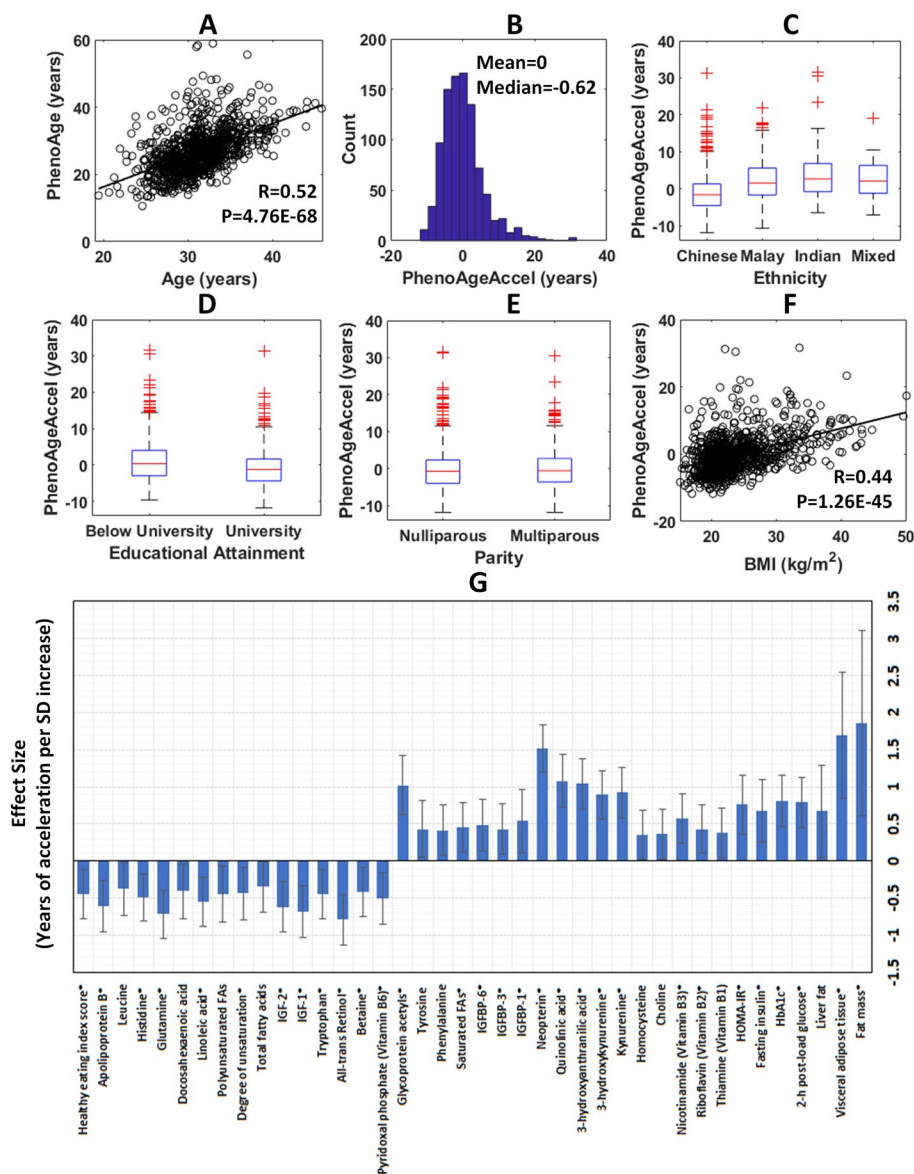


**Fig. 2** PhenoAgeAccel and its association results. **A** Phenotypic age vs. chronological age. **B** Histogram of PhenoAgeAccel. **C-E** Boxplots of ethnicity, educational attainment and parity with PhenoAgeAccel. **F** PhenoAgeAccel vs. BMI. **G** Effect size plot of 40 aging-related factors derived from multivariate analysis of clinical measurements and blood biomarkers with a nominal  $p$ -value  $< 0.05$ . \*:  $P_{adj} < 0.05$

associations were not significant after adjusting for covariates.

Out of the ten vitamins, pyridoxal-5-phosphate ( $\beta = -0.51$  and  $P = 3.43E-03$ ) and all-trans retinol ( $\beta = -0.79$  and  $P = 3.09E-06$ ) were inversely associated with PhenoAgeAccel while thiamine ( $\beta = 0.38$  and  $P = 2.33E-02$ ), riboflavin ( $\beta = 0.43$  and  $P = 1.08E-02$ ) and nicotinamide ( $\beta = 0.57$  and  $P = 8.81E-04$ ) showed a positive association with PhenoAgeAccel (Additional file 1: Table S2). Vitamin B12, folate and vitamin D showed a significant inverse association with PhenoAgeAccel

only in univariate analysis. No strong association was observed between alpha/gamma tocopherol and PhenoAgeAccel. Among the seven plasma one-carbon pathway metabolites, lower betaine ( $\beta = -0.42$  and  $P = 1.25E-02$ ) and higher choline ( $\beta = 0.36$  and  $P = 3.96E-02$ ) and homocysteine ( $\beta = 0.35$  and  $P = 3.94E-02$ ) levels were associated with higher PhenoAgeAccel (Additional file 1: Table S2). No association was observed for methionine. Dimethylglycine, cystathionine, and cysteine showed a positive association with PhenoAgeAccel only in univariate analysis. Association of plasma metabolites in

tryptophan metabolism with PhenoAgeAccel was studied (Additional file 1: Table S2). Tryptophan ( $\beta = -0.45$  and  $P = 8.25E-03$ ) showed an inverse association with PhenoAgeAccel. However, kynurenine ( $\beta = 0.92$  and  $P = 1.65E-07$ ), 3-hydroxykynurenine ( $\beta = 0.89$  and  $P = 1.47E-07$ ), 3-hydroxyanthranilic acid ( $\beta = 1.04$  and  $P = 3.80E-09$ ), quinolinic acid ( $\beta = 1.08$  and  $P = 1.61E-09$ ), and neopterin ( $\beta = 1.52$  and  $P = 3.92E-20$ ) exhibited a positive association with PhenoAgeAccel. There was no observed association for xanthurenic acid.

Associations of PhenoAgeAccel with plasma growth hormone and insulin-like growth factors were investigated (Additional file 1: Table S2). IGF-1 ( $\beta = -0.68$  and  $P = 1.61E-04$ ) and IGF-2 ( $\beta = -0.62$  and  $P = 5.04E-04$ ) exhibited an inverse association with PhenoAgeAccel while IGFBP-1 ( $\beta = 0.54$  and  $P = 1.39E-02$ ), IGFBP-3 ( $\beta = 0.43$  and  $P = 1.34E-02$ ) and IGFBP-6 ( $\beta = 0.48$  and  $P = 7.04E-03$ ) showed a positive association with PhenoAgeAccel. Among the plasma fatty acids, total FAs ( $\beta = -0.35$  and  $P = 4.33E-02$ ), degree of unsaturation ( $\beta = -0.44$  and  $P = 1.52E-02$ ), PUFAs ( $\beta = -0.45$  and  $P = 1.74E-02$ ), LA ( $\beta = -0.55$  and  $P = 1.21E-03$ ) and DHA ( $\beta = -0.41$  and  $P = 2.94E-02$ ) showed an inverse association with PhenoAgeAccel, whereas SFAs ( $\beta = 0.45$  and  $P = 7.94E-03$ ) exhibited a positive association with PhenoAgeAccel (Additional file 1: Table S2). Out of the plasma amino acids and proteins, higher plasma glutamine ( $\beta = -0.72$  and  $P = 1.31E-05$ ), histidine ( $\beta = -0.49$  and  $P = 3.02E-03$ ), leucine ( $\beta = -0.38$  and  $P = 3.69E-02$ ), and apolipoprotein B (ApoB) ( $\beta = -0.61$  and  $P = 4.88E-04$ ) concentrations were associated with lower PhenoAgeAccel, while higher plasma phenylalanine ( $\beta = 0.41$  and  $P = 1.83E-02$ ), tyrosine ( $\beta = 0.43$  and  $P = 2.63E-02$ ) and GlycA ( $\beta = 1.02$  and  $P = 7.44E-07$ ) concentrations were associated with higher PhenoAgeAccel (Additional file 1: Table S2). Overall, plasma neopterin displayed the strongest positive association ( $\beta = 1.52$ ) with PhenoAgeAccel, while plasma all-trans retinol demonstrated the strongest inverse association ( $\beta = -0.79$ ) in these 70 studied biomarkers.

In total, 40 aging-related factors ( $P < 0.05$ ) were derived from clinical measurements and blood biomarkers and are illustrated in Fig. 2G. Among them, 30 showed a strong association with a more stringent  $P_{\text{adj}} < 0.05$ .

### Multi-omics studies of PhenoAgeAccel

#### Plasma lipid signatures linked with PhenoAgeAccel

Association of plasma lipidomic profile with PhenoAgeAccel was investigated after the adjustment of age, ethnicity, educational attainment, parity and BMI. Out of 689 lipid species in 36 lipid classes, 132 showed significance with a nominal  $p$ -value threshold ( $P < 0.05$ ), and 16

demonstrated a strong association with a more stringent  $P_{\text{adj}} < 0.05$  (Additional file 2: Table S3 and Fig. 3A-B).

For neutral lipids, higher concentrations of acylcarnitines (AC(16:0)), triacylglycerol (TG(48:0) and TG(50:0)) and diacylglycerol (DG(16:0\_16:0)) with even-chain and saturated fatty acids were associated with higher PhenoAgeAccel, whereas odd-chain (AC(15:0), TG(O-54:4) [NL-17:1]) and unsaturated fatty acids (DG(18:2\_18:2), TG(52:4), TG(54:6) and TG(O-54:4) [NL-18:2]) were associated with lower PhenoAgeAccel (Fig. 3A). Six cholesterol ester species were inversely associated with PhenoAgeAccel regardless of chain length or unsaturation degree. Amongst these, CE(24:5) showed the strongest association ( $P = 1.36E-03$ ) with 0.93% decrease in concentration per year increase of age acceleration (Additional file 2: Table S3).

Out of the 32 aging-associated sphingolipids, 26 from ceramide (Cer), deoxy-ceramide (DeoxyCer), dihydroceramide (dhCer), sphingosine-1-phosphate (S1P), sphingosine (Sph), sphingomyelin (SM) and mono/di/trihexosylceramide (HexCer, Hex2Cer and Hex3Cer) lipid classes displayed a positive association with PhenoAgeAccel while only six lipid species (Cer(d19:1/24:0), Cer(d20:1/23:0), Cer1P(d18:1/16:0), GM3(d18:1/18:0), HexCer(d18:2/22:0)) and Hex3Cer(d18:1/18:0) showed an inverse association with it (Additional file 2: Table S3 and Fig. 3A). Amongst these, 7 lipids showed a strong association with  $P_{\text{adj}} < 0.05$  (Fig. 3B). Cer(d18:1/18:0) exhibited the strongest association ( $P = 3.77E-05$ ) with 0.93% increase in concentration per year increase of age acceleration.

For aging-associated phospholipids (PL), 51 lipid species from phosphatidylcholine (PC), alkylphosphatidylcholine (PC(O)), phosphatidylethanolamine (PE), alkyl/alkenylphosphatidylethanolamine (PE(O) and PE(P)), phosphatidylinositol (PI) and phosphatidylserine (PS) showed a positive association with PhenoAgeAccel. Conversely, 11 lipid species, including phosphatidylcholine (PC), alkenylphosphatidylcholine (PC(P)) and alkenylphosphatidylethanolamine (PE(P)) with odd-chain (PC(17:0\_18:2), PC(17:1\_18:2), PC(P-35:2), PC(P-17:0/20:4) and PE(P-17:0/22:6)) and branched-chain structures (PC(15-MHDA\_22:6)), as well as certain polyunsaturated fatty acids (PC(16:1\_22:6), PC(18:0\_22:6), PC(40:7) and PC(P-38:5)), displayed an inverse association with PhenoAgeAccel (Additional file 2: Table S3 and Fig. 3A-B). Amongst these, 5 phospholipids showed a strong association with  $P_{\text{adj}} < 0.05$  (Fig. 3B). PC(O-36:0) showed the strongest positive association ( $P = 2.03E-05$ ) by 1.26% increase in concentration per year increase of age acceleration, while PC(40:7) showed the strongest inverse association ( $P = 1.67E-03$ ) by 0.61% decrease in concentration per year increase of age acceleration.

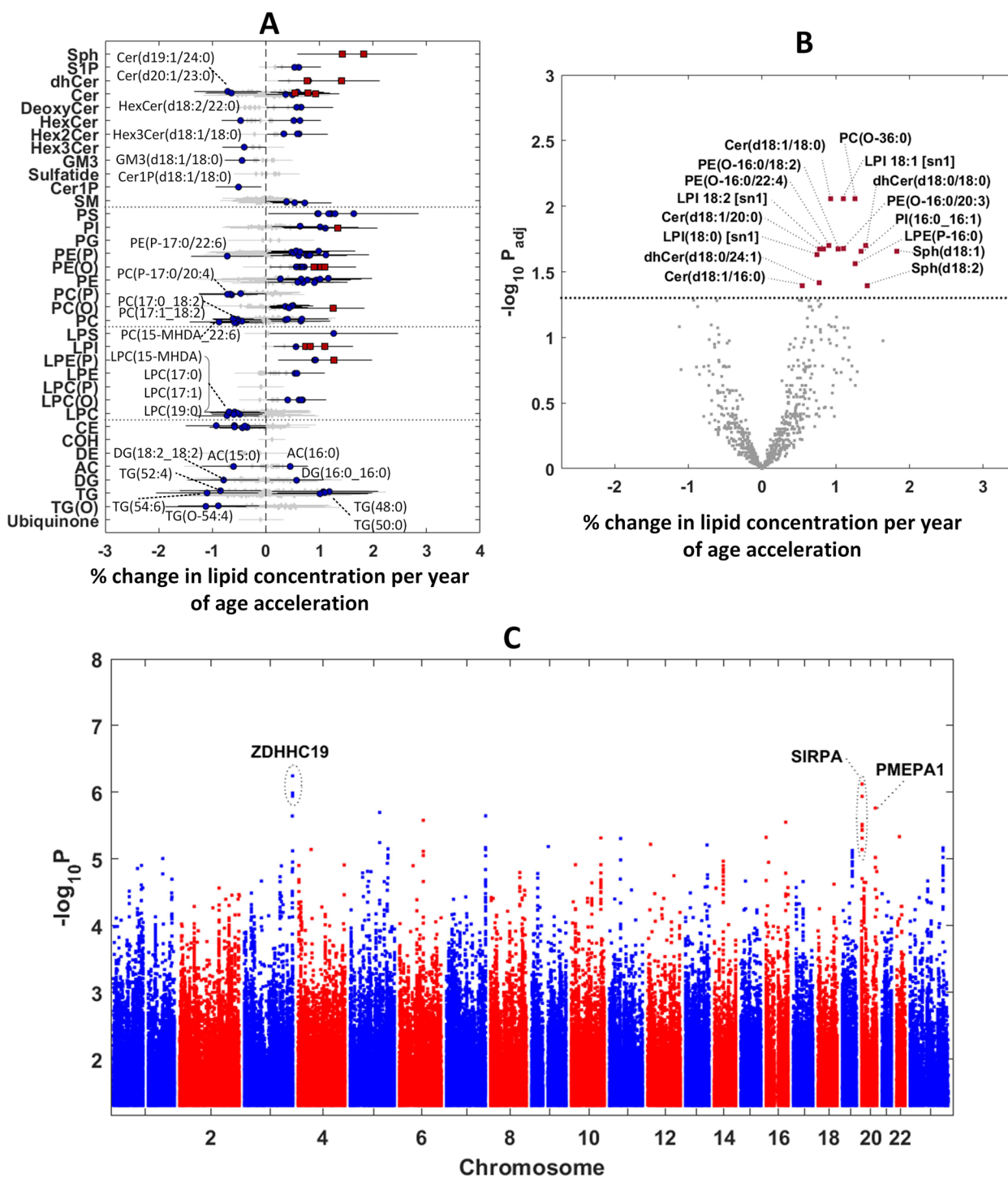


**Fig. 3** Lipidomics and GWAS results of PhenoAgeAccel. **A** Forest plot of lipidomics results. Diamond:  $P \geq 0.05$ , circle:  $P < 0.05$  and square:  $P_{adj} < 0.05$ . Full names of lipid classes are provided in Additional file 2: Table S3. **B** Volcano plots of lipidomics results. Lipid species with  $P_{adj} < 0.05$  are labelled. **C** Manhattan plot of the GWAS results. The top 3 mapped genes are labelled

Among the 20 aging-associated lysophospholipids, higher concentrations of lipid species from lysoalkylphosphatidylcholine (LPC(O)), lysophosphatidylethanolamine

(LPE), lysophosphatidylinositol (LPI) and lysophosphatidylserine (LPS) were associated with higher PhenoAgeAccel, whereas higher concentrations of

lysophosphatidylcholine (LPC) containing odd-chain (LPC(17:0), LPC(17:1) and LPC(19:0)) and branched-chain fatty acids (LPC(15-MHDA)) were associated with lower PhenoAgeAccel. Among those, four lysophospholipids showed a strong association with  $P_{\text{adj}} < 0.05$  (Fig. 3B). Overall, LPI(18:1) showed the strongest positive association ( $P = 3.82E-05$ ) by 1.10% increase in concentration per year increase of age acceleration while LPC(19:0) displayed the strongest inverse association ( $P = 3.73E-3$ ) by 0.69% decrease in concentration per year increase of age acceleration.

#### Genome-wide association study of PhenoAgeAccel

A genome-wide association study (GWAS) of PhenoAgeAccel was investigated after the adjustment of age and ethnicity. No genetic variants passed the typical threshold for genome-wide significance ( $P < 5.00E-08$ ). The quantile–quantile (Q-Q) plot are illustrated in Fig. S2. The genomic inflation factor of 1.02 indicated that the study exhibited very minor inflation and slight deviations in test statistics from the null distribution. A Manhattan plot was illustrated in Fig. 3C, highlighting the top 3 mapped genes (*ZDHHC19*, *SIRPA*, and *PMEPA1*). Boxplots were illustrated for the representative SNPs of the top 3 mapped genes (Additional file 1: Fig. S3A). The LocusZoom plots of *ZDHHC19*-rs9864994 and *SIRPA*-rs112608975 showed these two genes have multiple SNPs in LD (Additional file 1: Fig. S3B). The GWAS results of genetic variants with  $P < 1.00E-03$  were shown in Additional file 3: Table S4A and a list of genetic variants with synonymous or missense mutations were illustrated in Additional file 3: Table S4B. Interestingly, missense mutations of NADPH oxidase 4 (*NOX4*), interleukin 4 receptor (*IL4R*), defensins (*DEFB128* & *DEFB127*) and acyl-CoA synthetase bubblegum family member 2 (*ACSBG2*) were associated with PhenoAgeAccel.

For enrichment analysis, top 150 mapped genes (Additional file 3: Table S4C) from the GWAS results were analysed by Metascape (<https://metascape.org>) based on the following ontology sources: KEGG Pathway, GO Biological Processes, Reactome Gene Sets, Canonical Pathways, CORUM, WikiPathways, and PANTHER Pathway. Overall, top 20 clusters were found with their enriched terms with a  $p$ -value  $< 0.01$ , a minimum count of 3, and an enrichment factor  $> 1.5$  (Additional file 3: Table S4D). Their associated pathways included calcium ion transmembrane transport, ERBB2 activates PTK signaling, regulation of cardiac muscle cell contraction, apoptotic process involved in development, circadian entrainment, memory, regulation of phosphatase activity and Ras signaling pathway etc. (Additional file 1: Fig. S4).

In our study, we also performed a candidate analysis of the SNPs reported in the GWAS results of

PhenoAgeAccel from the UK biobank [18] and Taiwan biobank [15]. The results were shown in Additional file 3: Table S4E-F. Out of the 29 significant SNPs identified in the UK biobank, 26 SNPs were found in our SNP list after QC, with only two of them (*IL6R*-rs4129267:  $P = 9.87E-03$  and *FADS1/2*-rs174548:  $P = 2.85E-02$ ) showing weak associations (Additional file 3: Table S4E). Among the 11 significant SNPs identified in the Taiwan biobank, 8 SNPs remained in our SNP list after QC, with only one SNP (*AXINI*-rs7206286:  $P = 1.34E-02$ ) exhibiting a weak association (Additional file 3: Table S4F).

#### Gut microbiome association with PhenoAgeAccel

To explore the relationship between gut microbiome and PhenoAgeAccel, the alpha- and beta-diversity analysis were performed. PhenoAgeAccel was significantly inversely associated with 2 gut microbiome alpha-diversity measurements, Pielou's evenness and Faith's phylogenetic diversity (Additional file 1: Table S5). However, the significance was not retained after accounting for confounding factors, including BMI, age, ethnicity, educational attainment, and parity (Additional file 1: Table S5). Principal Coordinate Analysis (PCoA) based on Unweighted UniFrac distance, a metric measuring gut microbial community dissimilarity, demonstrated a statistically significant association with PhenoAgeAccel. Notably, this relationship remained significant even after adjusting for the aforementioned confounding variables ( $P_{\text{adj}} = 0.003$ , Fig. 4A and Additional file 1: Table S6).

To identify specific gut microbial species associated with PhenoAgeAccel, we employed a machine learning approach—nested cross-validated random forest regressor. This analysis identified the top 14 microbial species associated with PhenoAgeAccel, including *Streptococcus salivarius*, *Akkermansia*, Erysipelotrichaceae UCG-00, *Dorea*, *Enterococcus*, *Megasphaera*, *Dorea*, *Blautia*, *Lachnospirillum*, *Weissella*, *Allisonella*, *Massiliomicrobiota timonensis*, *Bifidobacterium*, and *Bacteroides vulgatus* (Fig. 4B). Out of these, three microbial species retained their significant associations with PhenoAgeAccel after comprehensive adjustment for BMI, age, ethnicity, educational attainment, and parity (Fig. 4C and Additional file 1: Table S7). Erysipelotrichaceae UCG-003 and *Bacteroides vulgatus* were significantly negatively associated with PhenoAgeAccel, whereas *Bifidobacterium* showed an inverse association (Fig. 4C).

#### Network analysis of aging-related factors

A schematic diagram was generated to illustrate the factors linked to accelerated biological aging based on association results from different platforms (Fig. 5A). Subsequently, 73 aging-related factors were selected for network analysis. These include 4 factors identified in



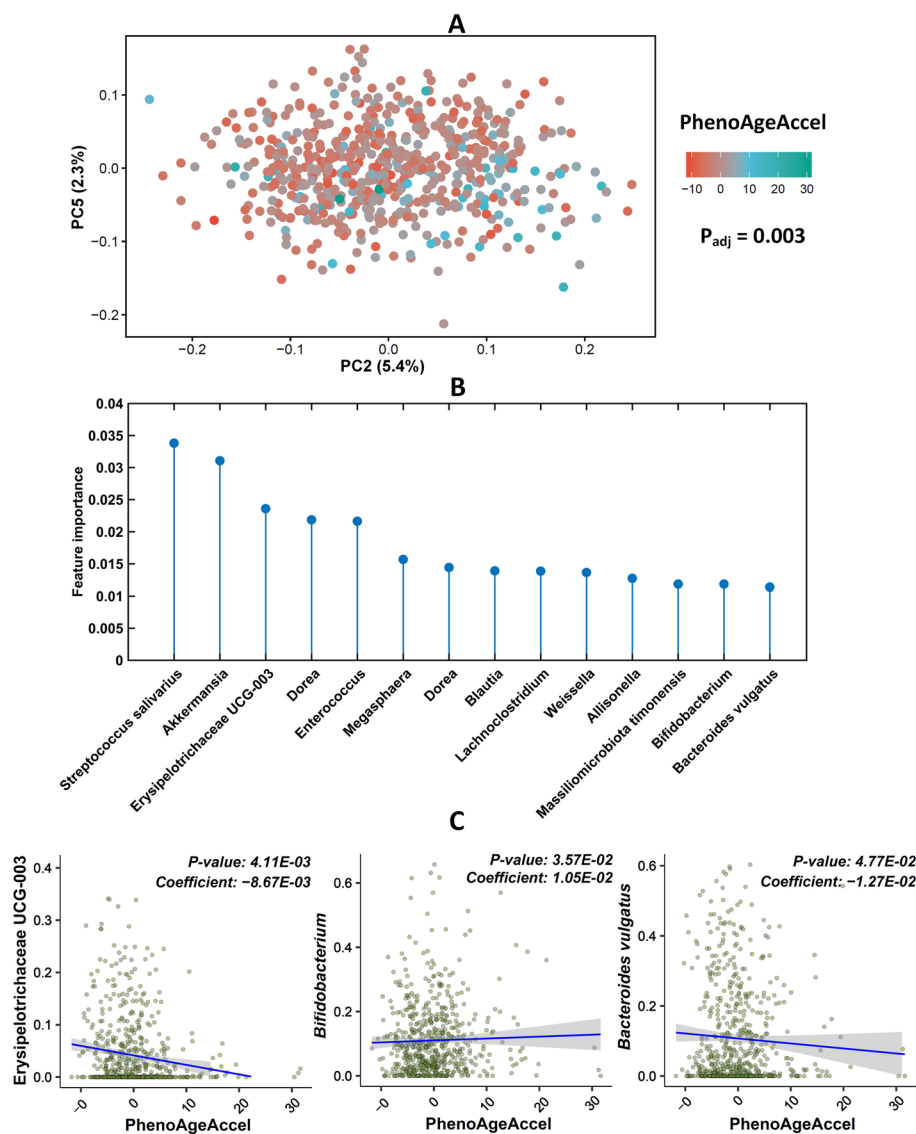


**Fig. 4** Association between the gut microbiome and PhenoAgeAccel. **A** Principal Coordinate Analysis of Unweighted UniFrac distance illustrating the gut microbiome of women with different PhenoAgeAccel.  $P_{adj}$  was obtained using multi-way ADONIS permutation-based statistical test after adjusting for the effects of ethnicity, BMI, age, educational attainment and parity. **B** The feature importance of the top 14 gut microbial species identified through nested cross-validated random forest regression. **C** Three microbial species significantly associated with PhenoAgeAccel identified via MaAsLin2 analysis

clinical measurements (Fig. 2G), and 36 blood biomarkers (Fig. 2G), 16 lipids ( $P_{adj} < 0.05$ , Fig. 3B), 3 representative SNPs of the top 3 mapped genes (*ZDHC19*, *SIRPA* and *PMEPA1*, Fig. S3A), and 14 gut microbial species (Fig. 4B). Firstly, to understand how these aging-related factors correlate with elements of PhenoAge (9 clinical biomarkers and CA), a network was generated based on their pair-wise correlation coefficients with  $|R| \geq 0.30$  (Additional file 1: Fig. S5). From this network,  $\ln(\text{CRP})$  was the element most strongly correlated with adiposity measures, glycaemic traits, FAs, lipid species, kynurenine

pathway metabolites, tyrosine, IGF-1, and GlycA, followed by white blood cell count and alkaline phosphatase, which also showing strong associations with these factors, except for lipid species, kynurenine pathway metabolites, tyrosine, and IGF-1. Fasting glucose was only strongly associated with glycaemic traits and adiposity measures. Albumin and creatinine were associated with fat mass and IGF-1, respectively.

Next, to explore the roles of aging-related factors derived from different platforms in the biological aging process, the interconnections among these factors

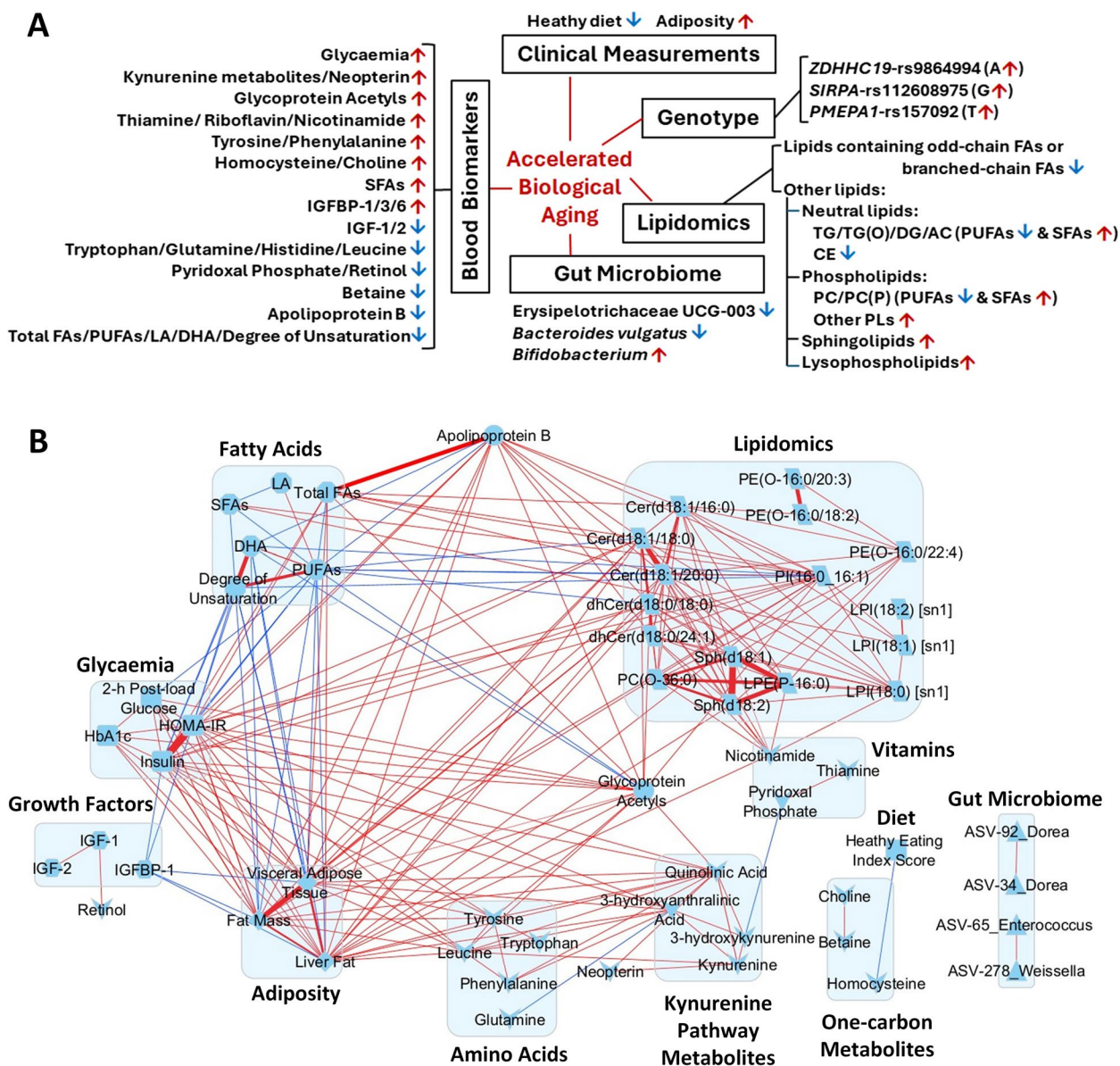


**Fig. 5** Network visualization of accelerated biological aging and aging-related factors. **A** Schematic diagram summarizing the factors linked to accelerated biological aging. **B** Network visualization of aging-related factors using Cytoscape. Each connection has a Spearman's rank correlation coefficient of  $\geq 0.30$ . Red – positive correlation and blue – negative correlation. Line width – magnitude of coefficient. These factors are grouped by their properties, denoted as different shapes of nodes

were investigated. The pairwise correlation heat map showed the overall connections between these factors with a  $p$ -value  $< 0.05$  (Additional file 1: Fig. S6). From the heatmap, adiposity measures, blood biomarkers and plasma lipid species showed a very strong interconnection among themselves but had a relatively weaker association with SNPs or gut microbial species. Of the 3 SNPs, ZDHC19-rs9864994 was inversely associated with IGF-1, IGF-2 and histidine, but positively

associated with Cer(d18:1/18:0) and *Lachnospirillum*. SIRPA-rs112608975 showed a positive association with thiamine, quinolinic acid and phenylalanine. PMEPA1-rs157092 exhibited a positive association with fat mass, liver fat, kynurenine pathway metabolites and 8 lipids from dihydroceramide, lysoalkenylphosphatidylethanolamine, lysophosphatidylinositol, alkylphosphatidylcholine, phosphatidylinositol and sphingosine while it showed an inverse association with HEI score, all-trans

retinol, plasma PUFAs, DHA, and degree of unsaturation. Among the three significant gut microbial species, Erysipelotrichaceae UCG-003, which showed an inverse association with PhenoAgeAccel, also exhibited a negative association with fat mass, liver fat, choline, SFAs and 6 lipids from dihydroceramide, alkylphosphatidylcholine, phosphatidylinositol and sphingosine. But it was positively associated with pyridoxal phosphate, PUFAs and 2 lipids from alkylphosphatidylethanolamine. Conversely, *Bifidobacterium*, which showed a positive association with PhenoAgeAccel, showed an inverse association with the HEI score, IGF-2, all-trans retinol and 3 amino acids (tryptophan, histidine, and leucine). Additionally, it was positively associated with homocysteine, neopterin, SFAs and 3 lipids from ceramide, lysoalkenylphosphatidylethanolamine and alkylphosphatidylcholine.

To simplify the complicated interconnections among these factors (Additional file 1: Fig. S6), only factors with  $|R| \geq 0.30$  were selected for network visualization (Fig. 5B). The 3 SNPs and 10 gut microbial species were not presented in the network due to their weak associations with other factors ( $|R| < 0.30$ ). The left 4 gut microbial species were kept only due to their strong interconnections among themselves. This integrative network highlighted complex correlations within and between categories of adiposity measures, blood biomarkers, and plasma lipid species. Several intriguing findings were observed. First, we observed strong correlations among adiposity measures, glycaemic traits, lipid-related components (such as fatty acids, ApoB, and lipids), and GlycA. Most of these correlations were positive, except for PUFAs, DHA, and degree of unsaturation, which were inversely associated with GlycA, lipids, adiposity and glycaemia. Second, IGFBP-1 exhibited a robust inverse relationship with adiposity measures, insulin, and HOMA-IR. Third, amino acids including leucine, tyrosine and phenylalanine displayed pronounced positive associations with adiposity measures, glycaemic traits, kynurenine pathway metabolites, and glycoprotein acetyls. Fourth, kynurenine pathway metabolites showed positive associations with glycaemic traits, adiposity measures, and GlycA. Fifth, nicotinamide (Vitamin B3) exhibited a strong positive connection with plasma lipids from sphingosine, ceramide, dihydroceramide, alkylphosphatidylcholine and lysoalkenylphosphatidylethanolamine. Lastly, homocysteine was inversely associated with HEI score.

#### Mediation effects of blood biomarkers

The influences of diet, adiposity, genetic variants, and gut microbial species on PhenoAgeAccel may be contributed through clinical biomarkers and circulating metabolites. Mediation analyses were performed for 10

predictors (HEI score, fat mass, liver fat, visceral adipose tissue, *ZDHHC19*-rs9864994, *SIRPA*-rs112608975, *PMEPA1*-rs157092, Erysipelotrichaceae UCG-003, *Bifidobacterium*, and *Bacteroides vulgatus*) and 36 mediators (aging-related blood biomarkers). Aging-related plasma lipid species were excluded due to their concurrent measurement with blood biomarkers, precluding causal inference. Additionally, plasma FA measures and ApoB were used as lipid biomarkers in this analysis. A total of 62 linkages (Fig. 6, Additional file 4: Table S8) were identified to mediate the associations between these predictors and PhenoAgeAccel through blood biomarkers ( $P_{ACME} < 0.05$ ), with 39 linkages remaining significant after multiple testing correction (Fig. 6,  $FDR < 0.2$ ).

HEI score was negatively associated with PhenoAgeAccel, mediated by multiple biomarkers related to lipid metabolism (DHA, SFAs, and degree of unsaturation), insulin/IGF signalling (insulin and IGF-1/2), immune activation and inflammation (tryptophan, neopterin, and 3-hydroxykynurenine), and nutritional metabolism (betaine, retinol, pyridoxal phosphate, thiamine, and riboflavin). The positive associations between adiposity measures (fat mass, liver fat, and visceral adipose tissue) and PhenoAgeAccel were mediated by multiple biomarkers linked to glucose metabolism (2-h post-load glucose, HbA1c, and HOMA-IR), insulin/IGF signalling (insulin, IGF-1 and IGFBP-6), immune activation and inflammation (kynurenine pathway metabolites and GlycA), nutritional metabolism (retinol and leucine), and lipid metabolism (LA, SFAs, and ApoB). For genetic variants, the association between *SIRPA*-rs112608975 and PhenoAgeAccel was mediated by biomarkers of immune activation and inflammation (neopterin and kynurenine) and insulin resistance (insulin and HOMA-IR), while the association between *ZDHHC19*-rs9864994 and PhenoAgeAccel was through IGF signalling (IGF2 and IGFBP-1). For *PMEPA1*-rs157092, neopterin and quinolinic acid were potential mediators. Among gut microbial species, neopterin strongly mediated the association between *Bifidobacterium* and PhenoAgeAccel. Additionally, multiple kynurenine pathway metabolites were identified as potential mediators for *Bacteroides vulgatus*, while IGF-1/IGFBP-6, LA, phenylalanine and nicotinamide were potential mediators for Erysipelotrichaceae UCG-003.

Furthermore, from the mediation results of 3 gut microbial species in the associations between 7 predictors (diet, adiposity, and genetic variants) and PhenoAgeAccel, only one significant linkage was identified with  $P_{ACME} < 0.05$ . Erysipelotrichaceae UCG-003 was found to mediate the association between fat mass and PhenoAgeAccel (Fig. 6B, Additional file 4: Table S8).



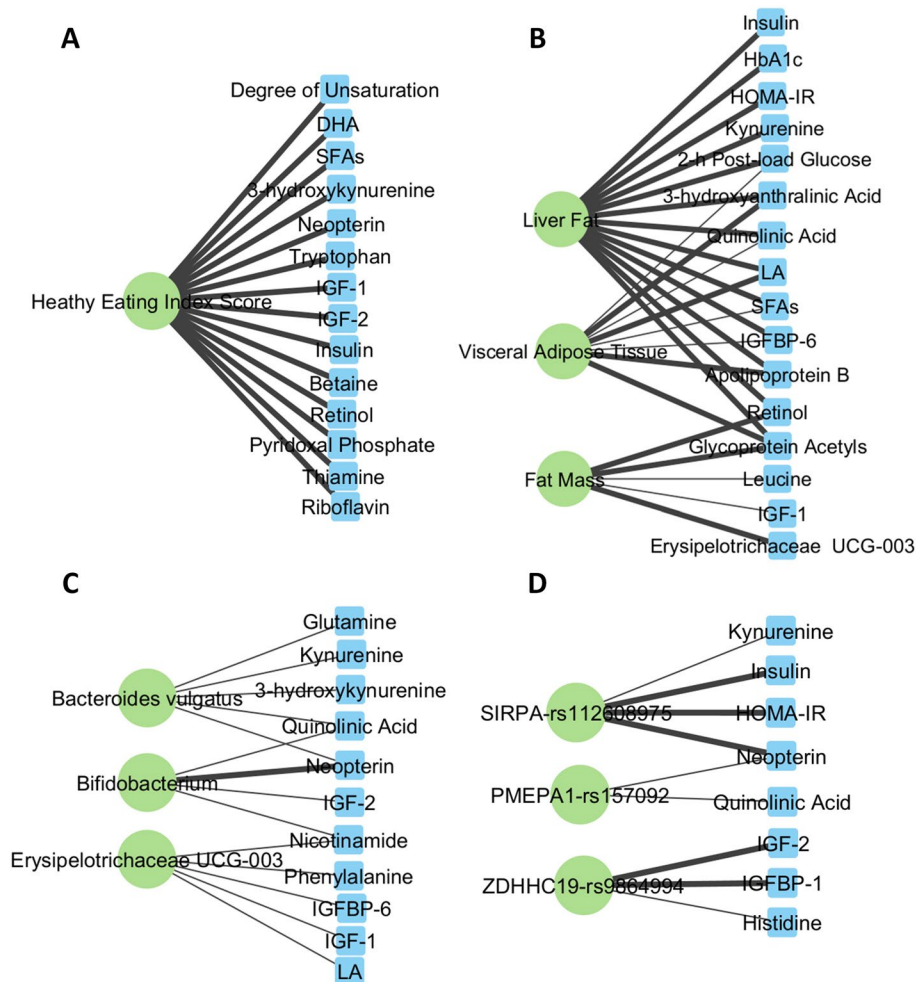


**Fig. 6** Effects of mediators (blue squares) on the associations between predictors (green circles) and the outcome (PhenoAgeAccel). **A** Diet (healthy eating index score). **B** Adiposity (Fat mass, liver fat and visceral adipose tissue). **C** Gut microbial species (Erysipelotrichaceae UCG-003, *Bacteroides vulgatus*, and *Bifidobacterium*). **D** Genetic variants (ZDHC19-rs9864994, SIRPA-rs112608975, and PMEPA1-rs157092). Age, ethnicity, educational attainment, parity and BMI were adjusted in analysis models. Each connection has a *p*-value of < 0.05 for average causal mediation effect (ACME), with a thicker line indicating an FDR of < 0.2

**Discussion**

To our knowledge, this is the first integrative study of clinical, nutritional, lipidomic, gut microbiome and genetic factors affecting biological age acceleration in Asian women of reproductive age. Signatures of lipidomics, gut microbiome and blood biomarkers in relation to PhenoAgeAccel were first reported. This study elucidates the physiological and molecular changes underlying biological aging and provides a comprehensive understanding of multi-systemic dysregulation that occurs in aging. We identified ethnic differences in PhenoAgeAccel in our cohort, where Indian and Malay women had higher PhenoAgeAccel than Chinese women. This is consistent with the trends in life expectancies in the different ethnic

groups in women in Singapore [43], and may be related to their socioeconomic status as women with higher educational attainment had lower PhenoAgeAccel. It may also be related to BMI as Indian and Malay women had higher BMI compared to Chinese women, and similar to other studies [44, 45], PhenoAgeAccel showed a very high correlation with BMI. The women in our study had a range of PhenoAgeAccel from -10 to > +20 years. Disparities in the pace of biological aging at midlife may have implications for future morbidity and mortality which may be reversed by interventions to alter reversible associated factors [4]. As the participants in this study (aged 18–45 years) are much younger than those in the other two Asian studies that look at PhenoAge (aged 35–90 and 30–70 years) [14, 15], this may contribute to the lower



correlation between PhenoAge and CA in this study compared to the other two studies.

Lifestyle factors have been reported to be associated with PhenoAgeAccel. Smoking accelerated biological aging [46], but good sleep quality [17], and healthy diet and regular physical activity [16] reduced accelerated aging. Alcohol consumption has been reported to be associated with epigenetic age acceleration [47]. As the women in the S-PRESTO cohort were recruited for attempting to conceive within the next 12 months, they were inclined to have an overall generally healthier lifestyle. This may be why we did not observe a strong association of PhenoAgeAccel with smoking (10% ever smoker) and alcohol consumption, physical activity, sleep duration and quality but just a strong inverse association with HEI score. This study found that multiple biomarkers related to insulin/IGF signalling, immune activation and inflammation, lipid metabolism, and nutritional metabolism mediated the association between HEI score and PhenoAgeAccel, highlighting the complex impact of diet on aging. Further, our cohort is relatively young compared to other studies e.g., the U.K. Biobank [17]. In lifestyle factors, diet is a strong factor consistently found in different studies to be associated with biological aging [48, 49]. In our study, depression and anxiety scores were not found to have a strong association with PhenoAgeAccel. Interestingly, the women who conceived within 12 months after recruitment had slightly lower PhenoAgeAccel than those who failed to conceive. However, the association was not retained after accounting for BMI, suggesting that BMI may play a more significant role in fecundability [50]. The accumulation of visceral fat is known to be associated with increased inflammation and metabolic diseases [51], which is in line with our observation that fat mass, visceral adipose tissue and liver fat were positively associated with PhenoAgeAccel. Strong mediating effects of multiple biomarkers related to glucose metabolism, insulin/IGF signalling, immune activation and inflammation, nutritional metabolism, and lipid metabolism were observed between adiposity and aging in this study.

Blood biomarkers serve as objective, quantifiable measures of physiological processes and pathological conditions within the body. This study investigated a broad spectrum of blood biomarkers including glycaemic status, lipid profile, liver enzymes, vitamins, one-carbon metabolites, tryptophan pathway metabolites, amino acids, growth factors, and inflammatory protein biomarkers. Among them, neopterin, a marker for immune system activation, showed the most significant association with PhenoAgeAccel. The production of neopterin is linked to the breakdown of tryptophan, and both activities are initiated by interferon-gamma, a pro-inflammatory

cytokine involved in immune functioning [52]. Increased degradation of tryptophan leads to the production of kynurenine pathway metabolites. We observed that tryptophan showed an inverse association with PhenoAgeAccel whereas kynurenine pathway metabolites such as kynurenine, 3-hydroxykynurenine, 3-hydroxyanthranilic acid and quinolinic acid were positively associated with PhenoAgeAccel. These results suggest that biological aging is associated with immune activation leading to enhanced tryptophan degradation and neopterin production. Among the one-carbon metabolites, choline was positively associated with age acceleration whereas betaine was associated with age deceleration. Betaine is an oxidative metabolite of choline and a methyl donor for converting homocysteine to methionine. It was reported that betaine suppressed pro-inflammatory signalling during aging [53]. The other two methyl donors, folate and vitamin B12, only showed a strong inverse association with accelerated aging in univariate analysis. Vitamin B6 also showed an inverse association with age acceleration. Deficiency of these B-vitamins have been linked with cognitive decline and subsequent oxidative damage [54]. As retinol (vitamin A) is known as an anti-inflammation vitamin because of its critical role in enhancing immune function [55], it logically demonstrated an inverse association with age acceleration. Surprisingly, nicotinamide, an NAD<sup>+</sup> (nicotinamide adenine dinucleotide) precursor, showed a positive association with aging in our study. However, other studies have shown increased nicotinamide with aging [56], implicating dysregulated NAD<sup>+</sup> metabolism in aging. Amino acids play a crucial role in various physiological processes in the body. It was observed that glutamine was inversely associated with accelerated aging as it has been reported to regulate the development of aging mediated by mTOR signaling and autophagy [57]. Histidine also exhibited an inverse association with accelerated aging, possibly because of its anti-glycating and free radical scavenging functions [58]. The opposite trends were observed in the association of age acceleration with leucine (negative), phenylalanine and tyrosine (positive) due to their different functions. High levels of tyrosine and phenylalanine were associated with insulin resistance [59] whereas leucine was an activator of the mTOR signalling pathway [60]. For protein biomarkers, GlycA was a stable inflammatory biomarker [61] which was positively associated with accelerated aging in this study. Higher ApoB level was associated with cardiovascular risk [62]. However, it only exhibited a positive association with age acceleration in a univariate analysis, but displayed an inverse association in a multivariate model, potentially attributed to collinearity with covariates. Low circulating IGF-1 has been associated with metabolic syndrome and increased

risk for cardiovascular disease and type 2 diabetes [63]. This is consistent with our observations that higher levels of growth factors (IGF-1 and IGF-2) and lower levels of their binding proteins (IGFBP-1, IGFBP-3 and IGFBP-6) were associated with decelerated biological aging.

Lipids play essential roles in regulating aging and longevity [64]. We did not find a strong association of the clinical serum lipid profile (total cholesterol, triglyceride, HDL-cholesterol and LDL-cholesterol) with biological aging after adjustment for covariates. However, we observed that high levels of saturated FAs and low levels of PUFAs (i.e., LA and DHA) were associated with accelerated aging in plasma FAs measures from <sup>1</sup>HNMR metabolomics. Furthermore, analysis of LC-MS/MS-based plasma lipidomics data provided an in-depth understanding of how specific lipid species linked to biological aging by examining 689 lipid species across 36 lipid classes. Out of 132 significant lipids, we found that lipid species with odd-chain FAs (i.e. 15:0, 17:0, 17:1 and 19:0) in acylcarnitines, phospholipids and lysophospholipids, and branched-chain FAs containing phospholipids were associated with slower biological aging. Odd-chain FAs are thought to be mainly derived from diet and microbiota. Decreased levels of branched-chain FAs have been associated with obesity [31] and the mechanism may be via alteration of gene expression in lipid synthesis and inflammation [65]. Plasma odd-chain FAs were inversely associated with type 2 diabetes risk and could potentially serve as biomarkers for dairy fat intake [66]. In phosphatidylcholine (PC), alkenylphosphatidylcholine (PC(P)) and glycerolipids (diacylglycerol, triacylglycerol and alkyldiacylglycerol), the lipid species with saturated FAs (i.e. palmitic and stearic acids) were associated with faster biological aging whereas the lipids with PUFAs (i.e. LA and DHA) were associated with slower biological aging. Saturated FAs were associated with obesity-related inflammation [67], whereas PUFAs (LA and DHA) were linked to anti-inflammatory effects [68]. Regardless of degree of unsaturation, cholesterol ester lipids were associated with slow biological aging, but phospholipids (i.e. PC(O), PE, PE(O), PE(P), PI and PS) were linked to accelerated aging. Esterification of cholesterol enables the safe and controlled storage and transportation of cholesterol, thereby helping to prevent the harmful effects of excess cholesterol in circulation [69]. Noteworthy, the performance of PC and PC(P) lipids was different from that of other phospholipids. Most sphingolipids (SPLs) were associated with accelerated biological aging, with ceramides showing the strongest association. Studies have indicated that elevated ceramide levels may be linked to an increased risk of cardiovascular disease events and diabetes, possibly due to the activation of NADPH oxidase and disruption of mitochondrial function [70].

These results highlighted the importance of investigating in-depth lipidomics in the context of aging research, extending beyond the standard clinical lipid profile.

Genetic factors are important contributors to biological aging [71]. GWAS of PhenoAgeAccel has been studied in participants of UK biobank aged 40–70 years and in participants of Taiwan biobank aged 30–70 years, respectively [15, 18]. Only one common SNP (*GCKR*-rs1260326,  $P < 5.00E-08$ ) was found in these two GWAS studies, but it was not significant in our study. We observed differences between the GWAS results of the UK biobank, Taiwan biobank and our S-PRESTO cohort, which could be due to different sample size, ethnicity ancestry, range of CA, the characteristics of cohorts. In our study, the participants were Asian women who were younger (age from 18–45 years old) and healthier than those in the other two studies. We did not observe any SNPs that passed genome-wide significance cutoff in our study, but some interesting findings still could be drawn from the top mapped genes and enrichment analysis. *ZDHHC19* (Zinc Finger DHHC-Type Palmitoyltransferase 19) belongs to a family of enzymes that play a crucial role in the process of protein palmitoylation, which regulates growth signalling (i.e., Wnt, AKT, and IGF-1/IGF1-R signalling) and immune function especially in partitioning immune signalling proteins to the membrane as well as to lipid rafts [72]. Interestingly, our results identified that two IGF signalling biomarkers mediated the association between *ZDHHC19*-rs9864994 and PhenoAgeAccel. *SIRPA* (Signal Regulatory Protein Alpha) is an immunoinhibitory receptor expressed by neutrophils, monocytes, macrophages, and dendritic cells (DC). Blockade of *SIRPA* leads to DC activation, macrophage phagocytosis and increased immune cell migration playing crucial roles in controlling inflammation responses [73]. *SIRPA* has been reported as part of a novel mechanism for inflammation-mediated insulin resistance in muscle [74]. Notably, this study identified that several biomarkers of immune activation, inflammation response, and insulin resistance mediated the association between *SIRPA*-rs112608975 and PhenoAgeAccel. *PMEPA1* (Prostate Transmembrane Protein, Androgen Induced 1) is induced by the TGF- $\beta$  signalling, but meanwhile, it inhibits the phosphorylation of Smad2 and Smad3 to antagonize TGF- $\beta$  signalling, which contributes to aging-related pathologies such as fibrosis and chronic inflammation and plays important roles in tissue repair and immune regulation. Our results found that two biomarkers of immune and inflammatory processes played a mediating role in the association between *PMEPA1*-rs157092 and PhenoAgeAccel. Enrichment results of top 150 mapped genes also showed the association with age-related pathways such as regulation of cardiac muscle cell contraction, apoptotic process

involved in development, circadian entrainment, memory, regulation of phosphatase activity and Ras signalling pathway.

The gut microbiome is associated with many age-associated changes, including immune system dysregulation and susceptibility to diseases [75]. In the current study, a compelling association between the gut microbiome and PhenoAgeAccel in women was unveiled, even after adjusting for covariates. Notably, our analysis identified two specific microbial species, Erysipelotrichaceae UCG-003 and *Bacteroides vulgatus*, which showed a significantly inverse association with PhenoAgeAccel. This finding is consistent with a previous study that highlighted the enrichment of Erysipelotrichaceae UCG-003 in the healthy aging cohort [76]. Moreover, several studies have consistently reported higher levels of Erysipelotrichaceae UCG-003 in the gut microbiome of healthy individuals when compared to patients afflicted with lung cancer [77] or colorectal cancer [78]. Intriguingly, our mediation analysis revealed that the association between Erysipelotrichaceae UCG-003 and PhenoAgeAccel was mediated by biomarkers related to IGF signalling, as well as nutritional and lipid metabolism. Erysipelotrichaceae UCG-003 was also found to mediate the association between fat mass and PhenoAgeAccel. Notably, Erysipelotrichaceae UCG-003 has been reported as a mediator in the association between body fat and the Energy-Adjusted Dietary Inflammation Index in the Multiethnic Cohort–Adiposity Phenotype Study [79]. *B. vulgatus*, on the other hand, has recently emerged as a promising microbe with potential health benefits. Supplementation with *B. vulgatus* Bv46 has demonstrated the capacity to ameliorate lipid metabolism in hyperlipidemic rats [80]. Consistent with recent findings in a study on cardiovascular disease risk and aging in the Chinese population, *B. vulgatus* was found to be negatively associated with aging in multimorbidity cluster 1, which was characterized by a relatively healthy metabolic profile [81]. Our study identified multiple kynurenine pathway metabolites as potential mediators in the association between *B. vulgatus* and PhenoAgeAccel, highlighting the mediating role of immune responses and inflammatory processes. Besides, one microbial species from *Bifidobacterium* was found to be positively associated with PhenoAgeAccel, with this association mediated by neopterin, a biomarker of inflammation. This suggests that this particular *Bifidobacterium* species may be linked to pro-inflammatory processes. While *Bifidobacterium* spp. are renowned for their beneficial effects in maintaining human health, recent studies have raised concerns about the potential invasiveness of certain *Bifidobacterium* species in immunocompromised hosts [82], which suggests the need for cautious investigation to better understand

the potential impacts of these specific *Bifidobacterium* species on health outcomes, using advanced approaches such as metagenomics or culturomics. Collectively, these findings underscore the promising potential of Erysipelotrichaceae UCG-003 and *B. vulgatus* in promoting healthy aging and sustaining overall well-being.

An integrative network analysis of aging-related factors provided a comprehensive overview of the underlying connections between them. Adiposity, glycaemic traits, and plasma factors, including FAs, lipids, amino acids, metabolites, and protein biomarkers, exhibited very strong correlations among themselves. Interestingly, the very strong positive association of nicotinamide with plasma lipids from sphingolipids and phospholipids may help to explain its accelerated effect on aging.

This study has several unique strengths. It offered an all-encompassing perspective on the relationship between PhenoAgeAccel and multi-platform data within a single study in women. This enabled us to evaluate aging-related factors from various angles to better understand the underlying mechanism. There are some limitations of this study. Sample size is relatively small for GWAS analysis in our study compared to two previously reported GWAS studies. Bias may exist in the self-reported variables (i.e. educational attainment, smoking status and alcohol consumption). This is a cross-sectional study with all assessments conducted at one time-point only so there remains limited understanding on the causal links, which is required to develop potential interventions to slow the aging process. Longitudinal studies would be needed to investigate aging trajectories based on different hallmarks in future studies. The women in our study are relatively young, hence the effects of aging-related factors may be blunted as compared to studies in older populations. However, we still have observed many significant associations with clinical, nutritional and lipidomics factors, suggesting that these factors play an important role in the variation of biological aging in Asian women of reproductive age.

## Conclusions

We investigated the association of PhenoAgeAccel with a range of multi-omics and clinical characteristics to reveal aging-related factors and performed integrative network and mediation analyses to better understand their biological connections and how they may underlie the aging process. We found that clinical factors, blood biomarkers, and lipids were interconnected, along with genetic variants and the gut microbiome, contributing collectively to biological aging. Moreover, blood biomarkers related to inflammation, immune response, and nutritional and energy metabolism potentially mediated the associations of diet, adiposity, genetic variants, and gut

microbial species with biological aging. These findings provide valuable insights into the molecular and metabolic mechanisms underlying biological aging. Potential interventions by targeting modifiable factors, including obesity, dietary choices, and specific nutrient intake, may help to mitigate accelerated biological aging, ultimately enhancing women's health. This study provides an important resource of aging research in Asian women and sheds light on the possibility of preventing the early onset of age-related diseases starting in young women.

#### Abbreviations

ACME	Average causal mediation effects
ALT	Alanine transaminase
AST	Aspartate transaminase
BMI	Body mass index
CA	Chronological age
CRP	C-reactive protein
DHA	Docosahexaenoic acid
EPDS	Edinburgh Postnatal Depression Scale
FA	Fatty acid
FPG	Fasting plasma glucose
2hPG	2-H post-load glucose
GGT	Gamma glutamyl transferase
GlycA	Glycoprotein acetyls
GWAS	Genome-wide association study
GWG	Gestational weight gain
HbA1c	Glycated haemoglobin
HDL	High-density lipoprotein
HEI	Healthy eating index
HOMA-IR	Homeostatic model assessment for insulin resistance
IGF	Insulin-like growth factors
IGFBP	Insulin-like growth factor binding protein
LA	Linoleic acid
LC-MS/MS	Liquid chromatography-tandem mass spectrometry
LDL	Low-density lipoprotein
MUFA	Monounsaturated fatty acid
NADPH	Nicotinamide adenine dinucleotide phosphate
NAD	Nicotinamide adenine dinucleotide
PhenoAge	Phenotypic age
PhenoAgeAccel	Phenotypic age acceleration
PL	Phospholipid
PSQI	Pittsburgh Sleep Quality Index
PUFA	Polysaturated fatty acid
PWR	Postpartum weight retention
SAT	Subcutaneous adipose tissue
SFA	Saturated fatty acid
SPL	Sphingolipid
STAI	State-Trait Anxiety Inventory
VAT	Visceral adipose tissue
AC	Acylcarnitine
CE	Cholesteryl ester
Cer	Ceramide
Cer1P	Ceramide-1-Phosphate
COH	Free cholesterol
DE	Dehydrocholesterol
deoxyCer	Deoxy-ceramide
DG	Diacylglycerol
dhCer	Dihydroceramide
GM3	GM3 ganglioside
HexCer	Monohexosylceramide
Hex2Cer	Dihexosylceramide
Hex3Cer	Trihexosylceramide
LPC	Lysophosphatidylcholine
LPC(O)	Lysoalkylphosphatidylcholine
LPC(P)	Lysoalkenylphosphatidylcholine

LPE	Lysophosphatidylethanolamine
LPE(P)	Lysoalkenylphosphatidylethanolamine
LPI	Lysoalkenylphosphatidylinositol
LPS	Lysophosphatidylserine
NL	Neutral loss
PC	Phosphatidylcholine
PC(O)	Alkylphosphatidylcholine
PC(P)	Alkenylphosphatidylcholine
PE	Phosphatidylethanolamine
PE(O)	Alkylphosphatidylethanolamine
PE(P)	Alkenylphosphatidylethanolamine
PG	Phosphatidylglycerol
PI	Phosphatidylinositol
PS	Phosphatidylserine
S1P	Sphingosine-1-Phosphate
Sph	Sphingosine
SM	Sphingomyelin
TG	Triacylglycerol
TG(O)	Alkyl-diacylglycerol

#### Supplementary Information

The online version contains supplementary material available at <https://doi.org/10.1186/s13073-024-01403-7>.

Additional file 1: Fig. S1: Chronological age, phenotypic age (PhenoAge) and PhenoAge acceleration (PhenoAgeAccel). Fig. S2 The QQ-plot in the GWAS analysis of PhenoAgeAccel. Fig. S3 The representative SNPs of the top 3 mapped genes in the GWAS results. Fig. S4 The top 20 clusters with their represented enriched terms using the top 150 mapped genes in the GWAS results by Metascape (<https://metascape.org>). Fig. S5 The association results of aging-related factors with elements of PhenoAge using Spearman's rank correlation analysis. Fig. S6 Pair-wise Spearman's rank correlation heat map of aging-related factors. Table S1 Clinical characteristics of chronological age and nine biomarkers for calculation of PhenoAge. Table S2 Linear regression results of clinical measurements and blood biomarkers with PhenoAgeAccel. Table S5 The association between alpha-diversity indices of the gut microbiome and PhenoAgeAccel. Table S6 Results of adonis test for phenotypic variables using the Unweighted Uni-Frac distance matrix of the gut microbiome. Table S7 Association between the top 14 microbial features and PhenoAgeAccel by using MaAsLin2.

Additional file 2: Table S3. The lipidomic results of PhenoAgeAccel after the adjustment of chronological age, ethnicity, educational attainment, parity and BMI.

Additional file 3: Table S4A. The GWAS results of PhenoAgeAccel. Table S4B A list of genetic variants with synonymous and missense mutations from the GWAS results in Table S4A. Table S4C The top 150 mapped gene for enrichment analysis. Table 4D The top 20 clusters with their enriched terms using the top 150 mapped genes by Metascape. Table S4E Candidate analysis in this study using the reported SNPs in the UK biobank. Table S4F Candidate analysis in this study using the reported SNPs in the Taiwan biobank.

Additional file 4: Table S8. Mediation results with PACME < 0.05 in the PhenoAgeAccel study.

#### Acknowledgements

We sincerely thank the study participants and S-PRESTO study group.

#### Authors' contributions

LC, KT, JX and JGE conceived and supervised the study. JSL, MTT, SC, SAS, NM, JY, SSV, ML, KHT, JC, MJM, SYC, YSC, PDG and JGE contributed to data and sample collection in S-PRESTO cohort. PM, SAM, MG, KN and BN involved in the discussion of result interpretation. LC, KT, and PM contributed to clinical data analysis. LC contributed to lipidomic analysis and GWAS. JX contributed to gut microbiome analysis. LC, KT and JX interpreted the results and wrote the manuscript. All authors read and approved the final manuscript.



### Funding

This research was supported by the Singapore National Research Foundation under its Translational and Clinical Research (TCR) Flagship Programme and administered by the Singapore Ministry of Health's National Medical Research Council (NMRC), Singapore- NMRC/TCR/004-NUS/2008; NMRC/TCR/012-NUHS/2014. Additionally, this research is supported by A\*STAR < C222812037 > and funding from the A\*STAR Institute for Human Development and Potential (A\*STAR IHDP).

### Data availability

Gut microbiome data has been archived to NCBI Sequence Read Archive (BioProject: PRJNA1154796) [83]. Lipidomics data [84] and genetic data [85] are accessible via Figshare. GWAS summary statistics are available via GWAS catalog [86]. The data supporting the findings and figures in this study are provided in the supplementary materials. Other data, including WGS data from the S-PRESTO cohort study are not publicly available due to multi-institutional cohort data governance and ethical restrictions. The S-PRESTO Executive Committee reviews the data access request and approves the distribution of data. Request for access can be sent to Png Hang (Png\_Hang@sics.a-star.edu.sg) for data access request submission-to-approval workflow. Please allow 10 working days for a response.

### Declarations

#### Ethics approval and consent to participate

The SingHealth Centralized Institutional Review Board granted ethical approval (reference 2014/692/D), written informed consent was obtained from all women. This study was conducted according to the guidelines laid down in the Declaration of Helsinki.

#### Consent for publication

Not applicable.

#### Competing interests

The authors declare that they have no competing interests.

#### Author details

<sup>1</sup>Institute for Human Development and Potential, Agency for Science, Technology and Research (A\*STAR), Singapore, Singapore. <sup>2</sup>Singapore Lipidomics Incubator, Life Sciences Institute, National University of Singapore, Singapore, Singapore. <sup>3</sup>Department of Laboratory Medicine, National University Hospital, Singapore, Singapore. <sup>4</sup>Department of Biochemistry, Yong Loo Lin School of Medicine, National University of Singapore, Singapore, Singapore. <sup>5</sup>Human Potential Translational Research Programme, Yong Loo Lin School of Medicine, National University of Singapore, Singapore, Singapore. <sup>6</sup>Department of Medicine and Human Potential Translational Research Programme, Yong Loo Lin School of Medicine, National University of Singapore, Singapore, Singapore. <sup>7</sup>Department of Endocrinology, Tan Tock Seng Hospital, Singapore, Singapore. <sup>8</sup>Lee Kong Chian School of Medicine, Nanyang Technological University, Singapore, Singapore. <sup>9</sup>Duke-NUS Medical School, Singapore, Singapore. <sup>10</sup>Department of Obstetrics and Gynaecology and Human Potential Translational Research Programme, Yong Loo Lin School of Medicine, National University of Singapore, Singapore, Singapore. <sup>11</sup>KK Women's and Children's Hospital, Singapore, Singapore. <sup>12</sup>Sackler Program for Epigenetics & Psychobiology, McGill University, Montréal, Canada. <sup>13</sup>Ludmer Centre for Neuroinformatics and Mental Health, Douglas Mental Health University Institute, McGill University, Montréal, Canada. <sup>14</sup>Folkhalsan Research Center, Helsinki, Finland. <sup>15</sup>Department of General Practice and Primary Health Care, University of Helsinki, Helsinki, Finland.

Received: 14 May 2024 Accepted: 29 October 2024

Published online: 08 November 2024

### References

- Lopez-Otin C, Blasco MA, Partridge L, Serrano M, Kroemer G. Hallmarks of aging: an expanding universe. *Cell*. 2023;186(2):243–78.
- DeVito LM, Barzilai N, Cuervo AM, Niedernhofer LJ, Milman S, Levine M, et al. Extending human healthspan and longevity: a symposium report. *Ann N Y Acad Sci*. 2022;1507(1):70–83.
- Whitty CJM, Watt FM. Map clusters of diseases to tackle multimorbidity. *Nature*. 2020;579(7800):494–6.
- Elliott ML, Caspi A, Houts RM, Ambler A, Broadbent JM, Hancox RJ, et al. Disparities in the pace of biological aging among midlife adults of the same chronological age have implications for future frailty risk and policy. *Nat Aging*. 2021;1(3):295–308.
- Gladyshev VN. Aging: progressive decline in fitness due to the rising deleteriousness of genetic, environmental, and stochastic processes. *Aging Cell*. 2016;15(4):594–602.
- Austad SN, Fischer KE. Sex differences in lifespan. *Cell Metab*. 2016;23(6):1022–33.
- Horvath S. DNA methylation age of human tissues and cell types. *Genome Biol*. 2013;14(10):R115.
- Jylhävä J, Pedersen NL, Hägg S. Biological age predictors. *EBioMedicine*. 2017;21:29–36.
- Liu Z, Kuo PL, Horvath S, Crimmins E, Ferrucci L, Levine M. A new aging measure captures morbidity and mortality risk across diverse subpopulations from NHANES IV: a cohort study. *PLoS Med*. 2018;15(12):e1002718.
- Levine ME. Modeling the rate of senescence: can estimated biological age predict mortality more accurately than chronological age? *J Gerontol A Biol Sci Med Sci*. 2013;68(6):667–74.
- Belsky DW, Caspi A, Houts R, Cohen HJ, Corcoran DL, Danese A, et al. Quantification of biological aging in young adults. *Proc Natl Acad Sci U S A*. 2015;112(30):E4104–10.
- Zhong X, Lu Y, Gao Q, Nyunt MSZ, Fulop T, Monterola CP, et al. Estimating biological age in the Singapore longitudinal aging study. *J Gerontol A Biol Sci Med Sci*. 2020;75(10):1913–20.
- Levine ME, Lu AT, Quach A, Chen BH, Assimes TL, Bandinelli S, et al. An epigenetic biomarker of aging for lifespan and healthspan. *Aging (Albany NY)*. 2018;10(4):573–91.
- Ma Q, Li BL, Yang L, Zhang M, Feng XX, Li Q, et al. Association between phenotypic age and mortality in patients with multivessel coronary artery disease. *Dis Markers*. 2022;2022:4524032.
- Lin WY. Lifestyle Factors and Genetic Variants on 2 Biological Age Measures: Evidence From 94 443 Taiwan Biobank participants. *J Gerontol A Biol Sci Med Sci*. 2022;77(6):1189–98.
- Thomas A, Belsky DW, Gu Y. Healthy lifestyle behaviors and biological aging in the U.S. National Health and Nutrition Examination Surveys 1999–2018. *J Gerontol A Biol Sci Med Sci*. 2023;78(9):1535–42.
- Gao X, Huang N, Guo X, Huang T. Role of sleep quality in the acceleration of biological aging and its potential for preventive interaction on air pollution insults: findings from the UK Biobank cohort. *Aging Cell*. 2022;21(5):e13610.
- Kuo CL, Pilling LC, Liu Z, Atkins JL, Levine ME. Genetic associations for two biological age measures point to distinct aging phenotypes. *Aging Cell*. 2021;20(6):e13376.
- Chen L, Liu R, Liu ZP, Li M, Aihara K. Detecting early-warning signals for sudden deterioration of complex diseases by dynamical network biomarkers. *Sci Rep*. 2012;2:342.
- Loo EXL, Soh SE, Loy SL, Ng S, Tint MT, Chan SY, et al. Cohort profile: Singapore Preconception Study of Long-Term Maternal and Child Outcomes (S-PRESTO). *Eur J Epidemiol*. 2021;36(1):129–42.
- Hildebrand M, Hees VTV, Hansen BH, Ekelund U. Age group comparability of raw accelerometer output from wrist- and hip-worn monitors. *Med Sci Sports Exerc*. 2014;46(9):1816–24.
- Buysse DJ, Reynolds CF 3rd, Monk TH, Berman SR, Kupfer DJ. The Pittsburgh sleep quality index: a new instrument for psychiatric practice and research. *Psychiatry Res*. 1989;28(2):193–213.
- Willett WC, Sampson L, Stampfer MJ, Rosner B, Bain C, Witschi J, et al. Reproducibility and validity of a semiquantitative food frequency questionnaire. *Am J Epidemiol*. 1985;122(1):51–65.
- Lim SX, Cox V, Rodrigues N, Colega MT, Barton SJ, Childs CE, et al. Evaluation of preconception dietary patterns in women enrolled in a multisite study. *Curr Dev Nutr*. 2022;6(7):nzac106.
- Tint MT, Ward LC, Soh SE, Aris IM, Chinnadurai A, Saw SM, et al. Estimation of fat-free mass in Asian neonates using bioelectrical impedance analysis. *Br J Nutr*. 2016;115(6):1033–42.

26. Provencher SW. Estimation of metabolite concentrations from localized in vivo proton NMR spectra. *Magn Reson Med*. 1993;30(6):672–9.
27. Szczepaniak LS, Nurenberg P, Leonard D, Browning JD, Reingold JS, Grundy S, et al. Magnetic resonance spectroscopy to measure hepatic triglyceride content: prevalence of hepatic steatosis in the general population. *Am J Physiol Endocrinol Metab*. 2005;288(2):E462–8.
28. Kway YM, Thirumurugan K, Michael N, Tan KH, Godfrey KM, Gluckman P, et al. A fully convolutional neural network for comprehensive compartmentalization of abdominal adipose tissue compartments in MRI. *Comput Biol Med*. 2023;167:107608.
29. Broekman BF, Chan YH, Chong YS, Kwek K, Cohen SS, Haley CL, et al. The influence of anxiety and depressive symptoms during pregnancy on birth size. *Paediatr Perinat Epidemiol*. 2014;28(2):116–26.
30. Matthews DR, Hosker JP, Rudenski AS, Naylor BA, Treacher DF, Turner RC. Homeostasis model assessment: insulin resistance and beta-cell function from fasting plasma glucose and insulin concentrations in man. *Diabetologia*. 1985;28(7):412–9.
31. Chen L, Mir SA, Bendt AK, Chua EWL, Narasimhan K, Tan KM, et al. Plasma lipidomic profiling reveals metabolic adaptations to pregnancy and signatures of cardiometabolic risk: a preconception and longitudinal cohort study. *BMC Med*. 2023;21(1):53.
32. Wu D, Dou J, Chai X, Bellis C, Wilm A, Shih CC, et al. Large-scale whole-genome sequencing of three diverse Asian populations in Singapore. *Cell*. 2019;179(3):736–49 e15.
33. Parada AE, Needham DM, Fuhrman JA. Every base matters: assessing small subunit rRNA primers for marine microbiomes with mock communities, time series and global field samples. *Environ Microbiol*. 2016;18(5):1403–14.
34. Apprill A, McNally S, Parsons R, Weber L. Minor revision to V4 region SSU rRNA 806R gene primer greatly increases detection of SAR11 bacterioplankton. *Aquat Microb Ecol*. 2015;75(2):129–37.
35. Xu J, Lawley B, Wong G, Ota A, Chen L, Ying TJ, et al. Ethnic diversity in infant gut microbiota is apparent before the introduction of complementary diets. *Gut Microbes*. 2020;11(5):1362–73.
36. Friedman J, Alm EJ. Inferring correlation networks from genomic survey data. *PLoS Comput Biol*. 2012;8(9):e1002687.
37. Quast C, Pruesse E, Yilmaz P, Gerken J, Schweer T, Yarza P, et al. The SILVA ribosomal RNA gene database project: improved data processing and web-based tools. *Nucleic Acids Res*. 2013;41(Database issue):D590–6.
38. Robeson MS 2nd, O'Rourke DR, Kaehler BD, Ziemski M, Dillon MR, Foster JT, et al. RESCRIPt: Reproducible sequence taxonomy reference database management. *PLoS Comput Biol*. 2021;17(11):e1009581.
39. Janssen S, McDonald D, Gonzalez A, Navas-Molina JA, Jiang L, Xu ZZ, et al. Phylogenetic placement of exact amplicon sequences improves associations with clinical information. *mSystems*. 2018;3(3):e00021–18.
40. Bokulich NA, Dillon MR, Bolyen E, Kaehler BD, Huttley GA, Caporaso JG. q2-sample-classifier: machine-learning tools for microbiome classification and regression. *J Open Res Softw*. 2018;3(30):934.
41. Mallick H, Rahnavard A, McIver LJ, Ma S, Zhang Y, Nguyen LH, et al. Multivariable association discovery in population-scale meta-omics studies. *PLoS Comput Biol*. 2021;17(11):e1009442.
42. Shannon P, Markiel A, Ozier O, Baliga NS, Wang JT, Ramage D, et al. Cytoscape: a software environment for integrated models of biomolecular interaction networks. *Genome Res*. 2003;13(11):2498–504.
43. Lim RB, Zheng H, Yang Q, Cook AR, Chia KS, Lim WY. Ethnic and gender specific life expectancies of the Singapore population, 1965 to 2009 - converging, or diverging? *BMC Public Health*. 2013;13:1012.
44. Hughes K, Yeo PP, Lun KC, Thai AC, Wang KW, Cheah JS. Obesity and body mass indices in Chinese, Malays and Indians in Singapore. *Ann Acad Med Singap*. 1990;19(3):333–8.
45. Zhang Y, Abidin E, Sambasivam R, Shafie S, Roystonn K, Vaingankar JA, et al. Changes in body mass index and its association with socio-demographic characteristics between 2010 and 2016 in Singapore. *Front Public Health*. 2024;12:1374806.
46. Simons RL, Ong ML, Lei MK, Klopach E, Berg M, Zhang Y, et al. Unstable childhood, adult adversity, and smoking accelerate biological aging among middle-age African Americans: similar findings for GrimAge and PoAm. *J Aging Health*. 2022;34(4–5):487–98.
47. Nannini DR, Joyce BT, Zheng Y, Gao T, Wang J, Liu L, et al. Alcohol consumption and epigenetic age acceleration in young adults. *Aging (Albany NY)*. 2023;15(2):371–95.
48. Kim Y, Huan T, Joehanes R, McKeown NM, Horvath S, Levy D, et al. Higher diet quality relates to decelerated epigenetic aging. *Am J Clin Nutr*. 2022;115(1):163–70.
49. Kresovich JK, Garval EL, Martinez Lopez AM, Xu Z, Niehoff NM, White AJ, et al. Associations of body composition and physical activity level with multiple measures of epigenetic age acceleration. *Am J Epidemiol*. 2021;190(6):984–93.
50. Loy SL, Cheung YB, Soh SE, Ng S, Tint MT, Aris IM, et al. Female adiposity and time-to-pregnancy: a multiethnic prospective cohort. *Hum Reprod*. 2018;33(11):2141–9.
51. Kolb H. Obese visceral fat tissue inflammation: from protective to detrimental? *BMC Med*. 2022;20(1):494.
52. Chen Y, Guillemin GJ. Kynurenine pathway metabolites in humans: disease and healthy States. *Int J Tryptophan Res*. 2009;2:1–19.
53. Go EK, Jung KJ, Kim JY, Yu BP, Chung HY. Betaine suppresses proinflammatory signaling during aging: the involvement of nuclear factor-kappaB via nuclear factor-inducing kinase/IkappaB kinase and mitogen-activated protein kinases. *J Gerontol A Biol Sci Med Sci*. 2005;60(10):1252–64.
54. An Y, Feng L, Zhang X, Wang Y, Wang Y, Tao L, et al. Dietary intakes and biomarker patterns of folate, vitamin B(6), and vitamin B(12) can be associated with cognitive impairment by hypermethylation of redox-related genes NUDT15 and TXNRD1. *Clin Epigenetics*. 2019;11(1):139.
55. Huang Z, Liu Y, Qi G, Brand D, Zheng SG. Role of vitamin A in the immune system. *J Clin Med*. 2018;7(9):258.
56. Clement J, Wong M, Poljak A, Sachdev P, Braidy N. The plasma NAD(+) metabolome is dysregulated in "Normal" Aging. *Rejuven Res*. 2019;22(2):121–30.
57. Zhou J, Chen H, Du J, Tai H, Han X, Huang N, et al. Glutamine availability regulates the development of aging mediated by mTOR signaling and autophagy. *Front Pharmacol*. 2022;13:924081.
58. Holecek M. Histidine in health and disease: metabolism, physiological importance, and use as a supplement. *Nutrients*. 2020;12(3):848.
59. Yamada C, Kondo M, Kishimoto N, Shibata T, Nagai Y, Imanishi T, et al. Association between insulin resistance and plasma amino acid profile in non-diabetic Japanese subjects. *J Diabetes Investig*. 2015;6(4):408–15.
60. Vellai T. How the amino acid leucine activates the key cell-growth regulator mTOR. *Nature*. 2021;596(7871):192–4.
61. Chiesa ST, Charakida M, Georgiopoulos G, Roberts JD, Stafford SJ, Park C, et al. Glycoprotein acetyls: a novel inflammatory biomarker of early cardiovascular risk in the young. *J Am Heart Assoc*. 2022;11(4):e024380.
62. Behbodikhah J, Ahmed S, Elyasi A, Kasselmann LJ, De Leon J, Glass AD, et al. Apolipoprotein B and cardiovascular disease: biomarker and potential therapeutic target. *Metabolites*. 2021;11(10):690.
63. Aguirre GA, De Ita JR, de la Garza RG, Castilla-Cortazar I. Insulin-like growth factor-1 deficiency and metabolic syndrome. *J Transl Med*. 2016;14:3.
64. Mutlu AS, Duffy J, Wang MC. Lipid metabolism and lipid signals in aging and longevity. *Dev Cell*. 2021;56(10):1394–407.
65. Czumaj A, Sledzinski T, Mika A. Branched-chain fatty acids alter the expression of genes responsible for lipid synthesis and inflammation in human adipose cells. *Nutrients*. 2022;14(11):2310.
66. Prada M, Wittenbecher C, Eichelmann F, Wernitz A, Drouin-Chartier JP, Schulze MB. Association of the odd-chain fatty acid content in lipid groups with type 2 diabetes risk: a targeted analysis of lipidomics data in the EPIC-Potsdam cohort. *Clin Nutr*. 2021;40(8):988–99.
67. Zhou H, Urso CJ, Jadeja V. Saturated Fatty acids in obesity-associated inflammation. *J Inflamm Res*. 2020;13:1–14.
68. Calder PC. Omega-3 fatty acids and inflammatory processes. *Nutrients*. 2010;2(3):355–74.
69. Griffiths WJ, Wang Y. Cholesterol metabolism: from lipidomics to immunology. *J Lipid Res*. 2022;63(2):100165.
70. Choi RH, Tatum SM, Symons JD, Summers SA, Holland WL. Ceramides and other sphingolipids as drivers of cardiovascular disease. *Nat Rev Cardiol*. 2021;18(10):701–11.
71. Melzer D, Hurst AJ, Frayling T. Genetic variation and human aging: progress and prospects. *J Gerontol A Biol Sci Med Sci*. 2007;62(3):301–7.
72. Li M, Zhang L, Chen CW. Diverse roles of protein palmitoylation in cancer progression, immunity, stemness, and beyond. *Cells*. 2023;12(18):2209.
73. Xie MM, Dai B, Hackney JA, Sun T, Zhang J, Jackman JK, et al. An agonistic anti-signal regulatory protein alpha antibody for chronic inflammatory diseases. *Cell Rep Med*. 2023;4(8):101130.

74. Thomas SS, Dong Y, Zhang L, Mitch WE. Signal regulatory protein- $\alpha$  interacts with the insulin receptor contributing to muscle wasting in chronic kidney disease. *Kidney Int.* 2013;84(2):308–16.
75. Badal VD, Vaccariello ED, Murray ER, Yu KE, Knight R, Jeste DV, et al. The gut microbiome, aging, and longevity: a systematic review. *Nutrients.* 2020;12(12):3759.
76. Singh H, Torralba MG, Moncera KJ, DiLello L, Petrini J, Nelson KE, et al. Gastro-intestinal and oral microbiome signatures associated with healthy aging. *Geroscience.* 2019;41(6):907–21.
77. Zhao F, An R, Wang L, Shan J, Wang X. Specific gut microbiome and serum metabolome changes in lung cancer patients. *Front Cell Infect Microbiol.* 2021;11:725284.
78. Park J, Kim NE, Yoon H, Shin CM, Kim N, Lee DH, et al. Fecal microbiota and gut microbe-derived extracellular vesicles in colorectal cancer. *Front Oncol.* 2021;11:650026.
79. Lozano CP, Wilkens LR, Shvetsov YB, Maskarinec G, Park SY, Shepherd JA, et al. Associations of the dietary inflammatory index with total adiposity and ectopic fat through the gut microbiota, LPS, and C-reactive protein in the multiethnic cohort-adiposity phenotype study. *Am J Clin Nutr.* 2022;115(5):1344–56.
80. Xu M, Lan R, Qiao L, Lin X, Hu D, Zhang S, et al. *Bacteroides vulgatus* ameliorates lipid metabolic disorders and modulates gut microbial composition in hyperlipidemic rats. *Microbiol Spectr.* 2023;11(1):e0251722.
81. Wang T, Shi Z, Ren H, Xu M, Lu J, Yang F, et al. Divergent age-associated and metabolism-associated gut microbiome signatures modulate cardiovascular disease risk. *Nat Med.* 2024;30(6):1722–31.
82. Esaïassen E, Hjerde E, Cavanagh JP, Simonsen GS, Klingenberg C. Norwegian study group on invasive bifidobacterial I. Bifidobacterium Bacteremia: clinical characteristics and a genomic approach to assess pathogenicity. *J Clin Microbiol.* 2017;55(7):2234–48.
83. Xu J. Gut microbiome vs. biological age acceleration. NCBI SRA. 2024; <http://www.ncbi.nlm.nih.gov/sra/PRJNA1154796>.
84. Chen L, Mir SA. S-PRESTO lipidomics data at preconception. Figshare. 2024; <https://doi.org/10.6084/m9.figshare.26830078.v1>.
85. Chen L. Three genetic variants for phenotypic age acceleration. Figshare. 2024; <https://doi.org/10.6084/m9.figshare.27308241.v1>.
86. Chen L. GWAS of genotypic age acceleration in Asian women. GWAS Catalog. 2024; <https://www.ebi.ac.uk/gwas/studies/GCST90454282>

## Publisher's Note

Springer Nature remains neutral with regard to jurisdictional claims in published maps and institutional affiliations.